Crimson Publishers
Wings to the Research

Review Article

Fracture Toughness, Mechanical Properties and Bending Behavior of AA1050/ Mg AZ31B Sheets Fabricated by an Accumulative Roll Bonding Technique

Payam Tayebi and Ramin Hashemi*

School of Mechanical Engineering, Iran University of Science and Technology, Iran

ISSN: 2640-9690

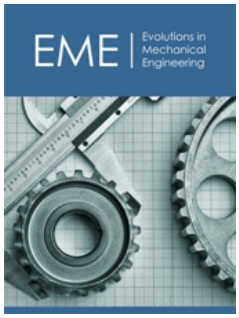

***Corresponding author:** Ramin Hashemi, School of Mechanical Engineering, Iran University of Science and Technology, Iran

Submission: July 12, 2024
Published: July 25, 2024

Volume 5 - Issue 4

How to cite this article: Payam Tayebi and Ramin Hashemi*. Fracture Toughness, Mechanical Properties and Bending Behavior of AA1050/ Mg AZ31B Sheets Fabricated by an Accumulative Roll Bonding Technique. Evolutions Mech Eng. 5(4). EME.000616. 2024.
DOI: 10.31031/EME.2024.05.000616

Abstract

In this article, Accumulative Roll Bonding (ARB) of AA 1050/AZ31B/AA 1050 sheets was performed up to the third pass and the fracture toughness for the different passes was experimentally studied for the first time. The mechanical properties, fracture behavior, and microstructure were determined through the tensile test, micro-hardness, plane stress fracture toughness, Optical Microscopy (OM), and Scanning Electron Microscopy (SEM). Due to the importance of the penetration layer depth of the ARBed samples, the effect of annealing temperature on the penetration layer depth was carried out at three annealing temperatures of 200°, 300°, and 400°. The results of the Scanning electron microscopy equipped with energy-dispersive X-ray spectroscopy (SEM-EDX) test showed that increasing the annealing temperature for the rolled sample of pass 1-3 increases the penetration depth. The fracture toughness of the ARBed samples was improved as the ARBed pass number was increased (e.g., the fracture toughness of the third pass was 32% more than the first pass). This improvement was observed for the ARBed samples compared to the base sheets (e.g., the fracture toughness of the 3rd-pass ARBed sample was 51% and 111% more than aluminum and Mg base sheets, respectively).

Keywords: AA1050/Mg AZ31B sheets; Accumulative Roll Bonding (ARB); Fracture toughness; Annealing temperature effect; Mechanical properties

Introduction

The increase in fuel costs and the growing pollution problem in big cities worldwide have led the production towards using lightweight metals. Recently, the use of metals with a high strength-to-weight ratio has risen in various industries. Aluminum and Mg are widely used metals in today's industries. One of the advantages of composite mg with Al is that while maintaining the low density of Mg, its ductility and corrosion resistance increase. The applications of lightweight alloys can be mentioned in the military and aerospace industries [1]. It is predicted that in the future, about 40 to 100kg of Mg will be used in the construction of most cars [2]. Considering that there are different methods for producing composites with ultra-fine grain structure, the ARB method, one of the Severe Plastic Deformations (SPD) methods, is of interest due to its economic advantages [3]. One of the benefits of producing multilayered sheets with the ARB method is the production of high-strength samples [4-6]. Sarvi et al. [7] evaluated three different routes: normal, reverse, and cross-on mechanical properties of the Al ARB sample. They showed that the mechanical properties will improve in the expected direction. Cheepu et al. [8] investigated the effects of the microstructure of the ARBed Al/Mg/Al sample. They showed that the intermetallic phase is formed at the Intersection. Habila et al. [9] showed that the mechanical properties of Al/Mg/Al sheets produced by the ARB process decrease after the third pass. Chen et al. [10] used the ARB process to fabricate the Al/Mg sample to pass 3. They reported that the hardness of the samples increases with the increase in the number of ARB passes.

Wu et al. [11] fabricated ARBed Al/Mg up to the third pass and then checked the metallurgical and mechanical properties of the specimens. Chang et al. [12] studied the influence of the strain on the penetration depth and found that the layers' penetration depth increases with the increase of applied rolling strains. Liu et al. [13] examined the mechanical and metallurgical properties of the 3-layer AL/Mg/AL samples produced by the ARB process up to the third pass. They showed that the grain size becomes refined with the increase in the rolling pass number. Weiying et al. [14] studied the influence of the number of passes of the ARB process for the Al-Mg sheet and found that an increase in the pass number of the rolling process leads to a better penetration of the layers. Zhang et al. [15] investigated ARB with two common methods using a hard plate. The results showed that when a hard plate is used in ARB, the connection conditions will improve. Alizadeh et al. [16] investigated the effect of the number of ARB passes on the tensile strength of the ARBed samples and showed that by increasing the number of ARB passes from one to seven passes, the strength will increase.

Taherian et al. [17] investigated the corrosion of Al 1100 and Al 6061 produced by the ARB process and showed that the rolled 6061 sample has higher corrosion resistance. Esmaeilzadeh et al. [18] studied the effect of the ARB number passes for Al/Cu/Br and investigated the corrosion behavior and microstructure. They found that the Cu layer fractured after the second ARB passed in the Al matrix. They showed that the wear rate will decrease significantly with the increase in the ARB number of passes. Sun et al. [19] investigated the effect of the ARB number passes and annealing temperature on the mechanical properties of Zn/Cu. The results showed that by increasing the rolling pass up to the 14th pass, the strength increases and by performing the annealing process at 150 °C for 10 minutes, the final strength will decrease. This article investigated fracture toughness and strength in three-point bending for ARBed sheets up to the third pass. Then, considering the annealing temperature effect, the mechanical and microstructural properties of the ARBed samples were evaluated. The effect of the ARB pass number on crack growth resistance in the fracture toughness test and quantitative studies related to XRD by MAUD software for ARB samples was investigated for the first time.

Experimental Procedure

Materials and ARB procedure

This research used AA1050 with 1mm thickness and AZ31B with 1mm thickness to produce an Al/Mg composite. The samples were prepared with AA 1050/ AZ31B/ AA 1050 arrangement according to Figure 1 with dimensions of 130x70mm to carry out the ARB process. Due to the brittleness of the Mg structure, to prevent cracking and breaking of the rolled sample, the prepared sample is preheated for 10 minutes at 400 °C after the etch pass, and then the rolling process is carried out. After the preparation of the samples in the first ARB pass, rolling was done with an AA 1050/AZ31B/AA 1050 arrangement. Then, by cutting the samples in the first pass and re-preparing them, the rolling process was done until the third pass. The layers' total number was calculated by 2n+1+1, where n is the number of ARB cycles. The percentage of thickness reduction in each rolling pass is considered to be 50% [20].

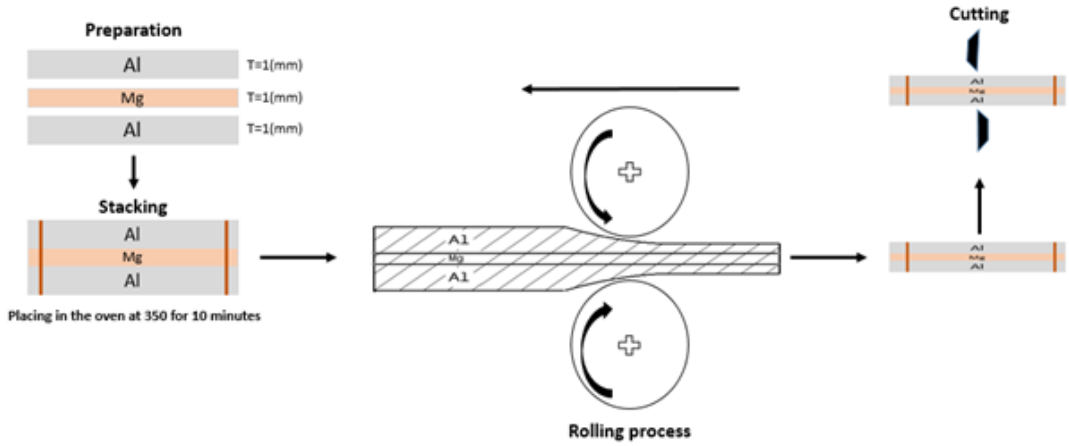

Figure 1: Schematic illustration of the ARB process.

Annealing and microstructure process

In order to remove the effect of residual stresses caused by the rolling process, annealing is done. The effect of the annealing process on the mechanical and metallurgical properties of the ARB samples was investigated. The annealing process was carried out at three temperatures of 200, 300, and 400 °C for 1.5 hours in the furnace [21]. For the Al/Mg composite, if the annealing temperature is below 200 °C, no intermetallic phase will be formed in the infiltration layer. If the annealing temperature exceeds 400 °C, the infiltration layer can melt at the interface. During the annealing process, after the ARB process, three different phenomena will occur, and the effect of each of these phenomena on layers bond strength will be investigated [22]:

A. The annealing operation will reduce the hardness of the sheet, and as a result, the toughness of the bond will increase. In this case, the force required for crack growth increases, and bond strength increases.

B. The annealing process, the residual stress in the penetrating layer decreases or disappears, in which case the bonding strength will increase.

C. The phenomenon of the brittle intermetallic phase formation in the penetration zone will decrease the bonding strength

According to the explanations mentioned above, if the effect of the intermetallic phase formation is more significant than in the other two cases, it causes the bond strength and, consequently, the tensile strength of the multilayer samples to decrease. As a result, the effort is to create conditions at different annealing temperatures that increase the depth of penetration and bond strength, and the tensile strength does not decrease. The EDS-Line and map test was performed to investigate the effects of annealing temperature on the penetration depth of Al-Mg layers. X-Ray Powder Diffraction (XRD) with grazing method and 20° to 80° was also performed to check the intermetallic phases formed in the ARB samples. FESEM images were used to evaluate the fracture morphology from tensile fractured surfaces.

Mechanical properties

Because after the ARB process, a new combination of multilayer Al-Mg sheets is formed, it is necessary to check the mechanical properties of the ARB in 4 temperature conditions: ambient, 200 °C, 300 °C and 400 °C. The tensile test was prepared by the ASTM-E8M standard by a single-axis tensile machine with a speed of 2mm/min (Figure 2(a)). Vickers hardness test was performed for ARBed samples in 3 zones A, B and C. Micro-hardness test was done with the applied load of 100gr for 15s (Figure 2(b&c)) [23]. However, the three-point bending and fracture toughness test was conducted only at ambient temperature to investigate the effect of the ARB process compared to the base sheets. The fracture toughness test was done according to the standard ASTM-E 647 [24] and with a 0.5mm/min test rate. The equipment and sample size used are shown in Figure 3(a&b). A three-point bending test was performed by applying pressure force and a 0.5mm/min displacement rate (Figure 3(c)).

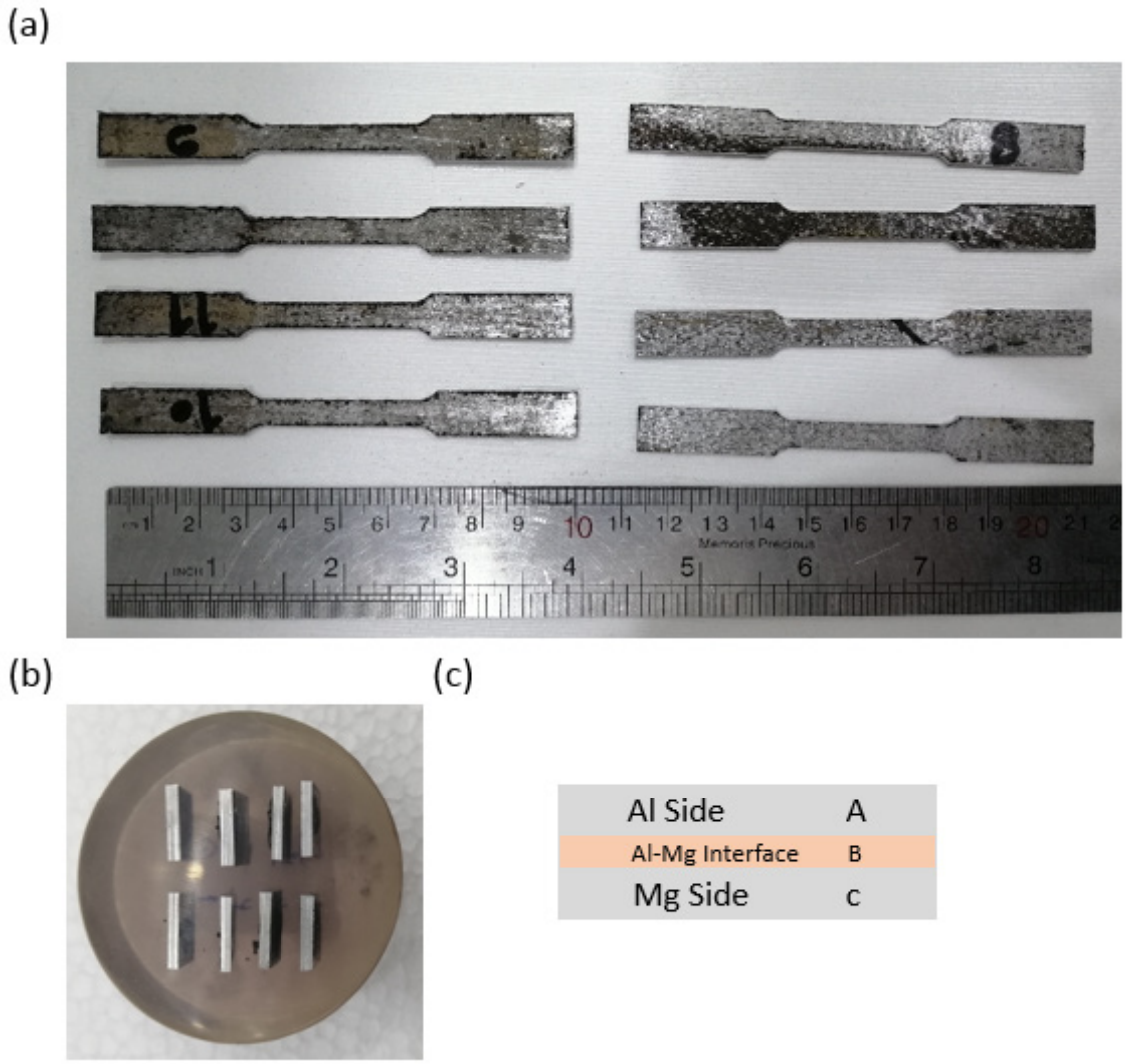

Figure 2: (a) Prepare tensile test, (b) Mount sample preparation for hardness testing, (c) Hardness measurement points.

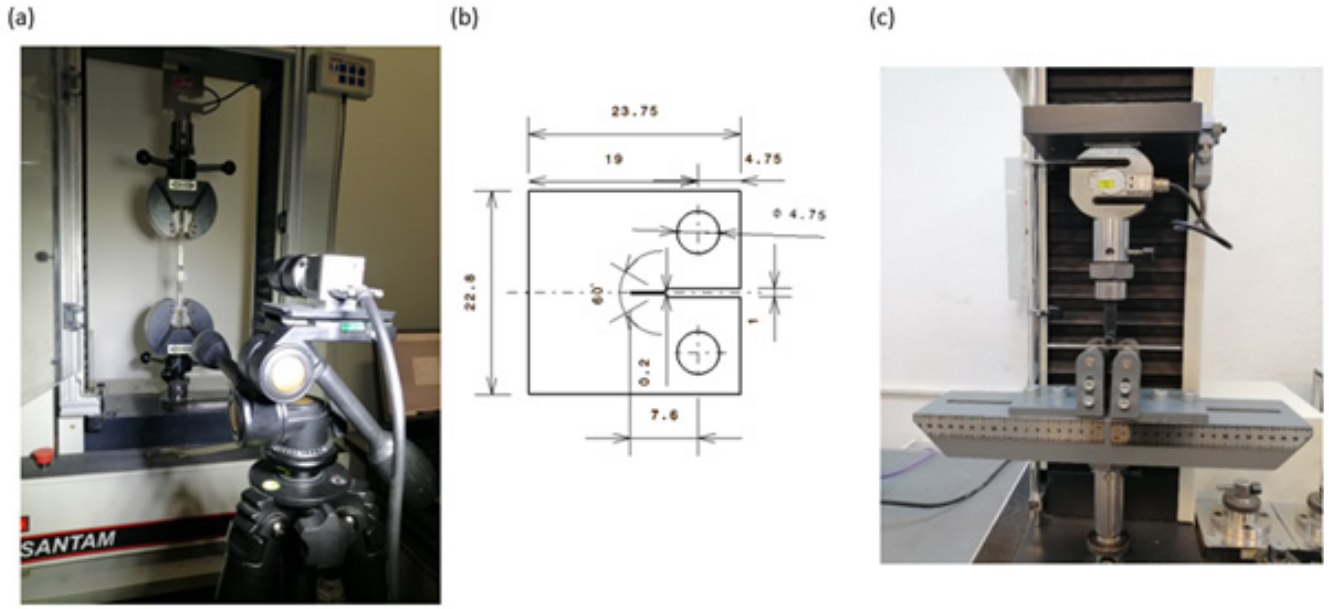

Figure 3: (a) The setup of fracture toughness test, (b) Sample size prepared for fracture toughness test, (c) three-point bending.

Result and Discussion

This section will investigate the effect of annealing temperature on the tensile test samples' mechanical and metallurgical properties of the ARB samples. Considering that after each rolling pass, the mechanical and metallurgical properties of the multilayer sample were changed, and considering the industrial applications foreseen for this method, according to analyses carried out in this part, the best conditions for annealing temperature will be reviewed and reported. The mechanical properties and Microstructural examination of the ARBed samples in pass 1-3 in 4 different temperature conditions and the Al and Mg base sheets at ambient temperature were performed by uniaxial tensile test, micro-hardness, fracture toughness and 3-point bending.

Uniaxial tensile study

The results of the tensile test can be seen in Figure 4. Tensile test results show an increase in strength with an increase in the number of passes in the Al/Mg composite. This shows that in both metals, due to the crystal structure of Al (FCC) and Mg (HCP), increasing the dislocations density results in a composite with a higher strength. On the other hand, by examining the effect of annealing temperature, it is observed that increasing the annealing temperature causes a decrease in the strength of the composite structure. The most significant reduction of the strength of the Al/Mg composite occurs at a temperature of 300 °C and above. Among the reasons for this decrease in strength are the recrystallization and growth of new grains and the decrease in the density of dislocations due to the annealing process [25]. The amount of strain at the temperature of 200 °C increases compared to the ambient temperature. This indicates that up to a temperature of 200 °C, due to the increase in the grain size and, as a result, the hardness decreases, as well as decreases of the dislocations density, the sample will decrease in strength and increase in formability.

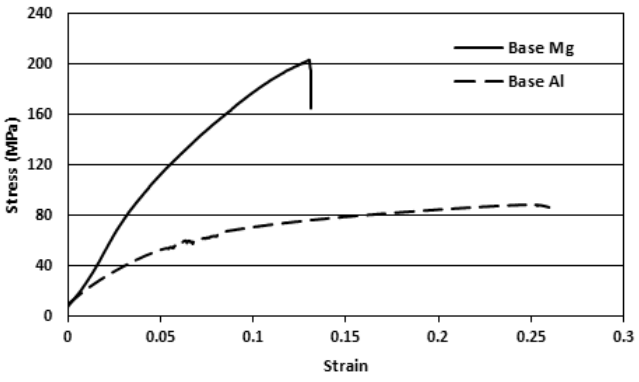

(a)

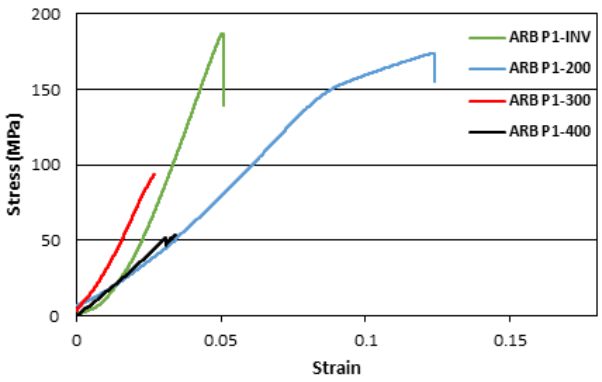

(b)

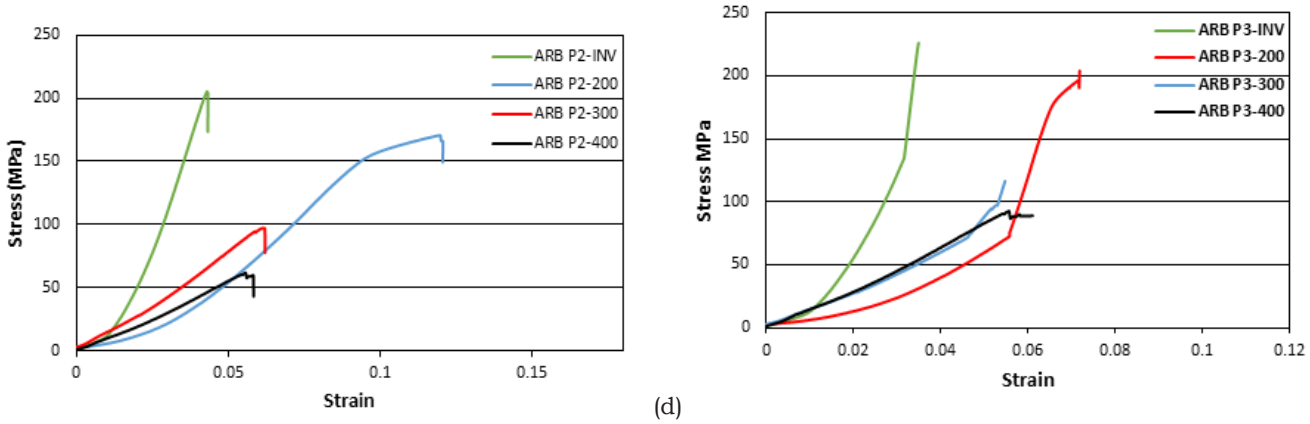

Figure 4: Uniaxial tensile test results in four different temperature conditions: (a) Base sheets, (b) ARB pass 1, (c) ARB pass 2, (d) ARB pass 3.

On the other hand, the more the annealing temperature goes up, the lower the amount of strain becomes, which can be attributed to the creation of intermetallic phases. One of the factors that affect the strain of the multilayer sample is the residual stress. Due to the different thermal expansion coefficients of these phases, during cooling and even heating, in the Intersection of different phases, residual stress is created, which hurts the amount of strain. Among the other reasons for the reduction of bond strength with increasing temperature, we can mention an important penetration mechanism called the Kirkendall effect. In this case, the voids move against the direction of movement of atoms and accumulate in the form of tiny holes, which causes that during the tensile test, these defects act as areas of stress concentration and cause crack propagation and failure [26].

Micro-hardness study

Vickers micro-hardness test was performed in 4 different temperature conditions for base sheet samples and ARBed sheets for passes 1 to 3. The results are shown in Figure 5. By comparing the micro-hardness test results, it can be seen that increasing the number of rolling passes increases the hardness, and increasing the annealing temperature decreases the hardness. By carefully studying the obtained results, in general, the following results can be obtained:

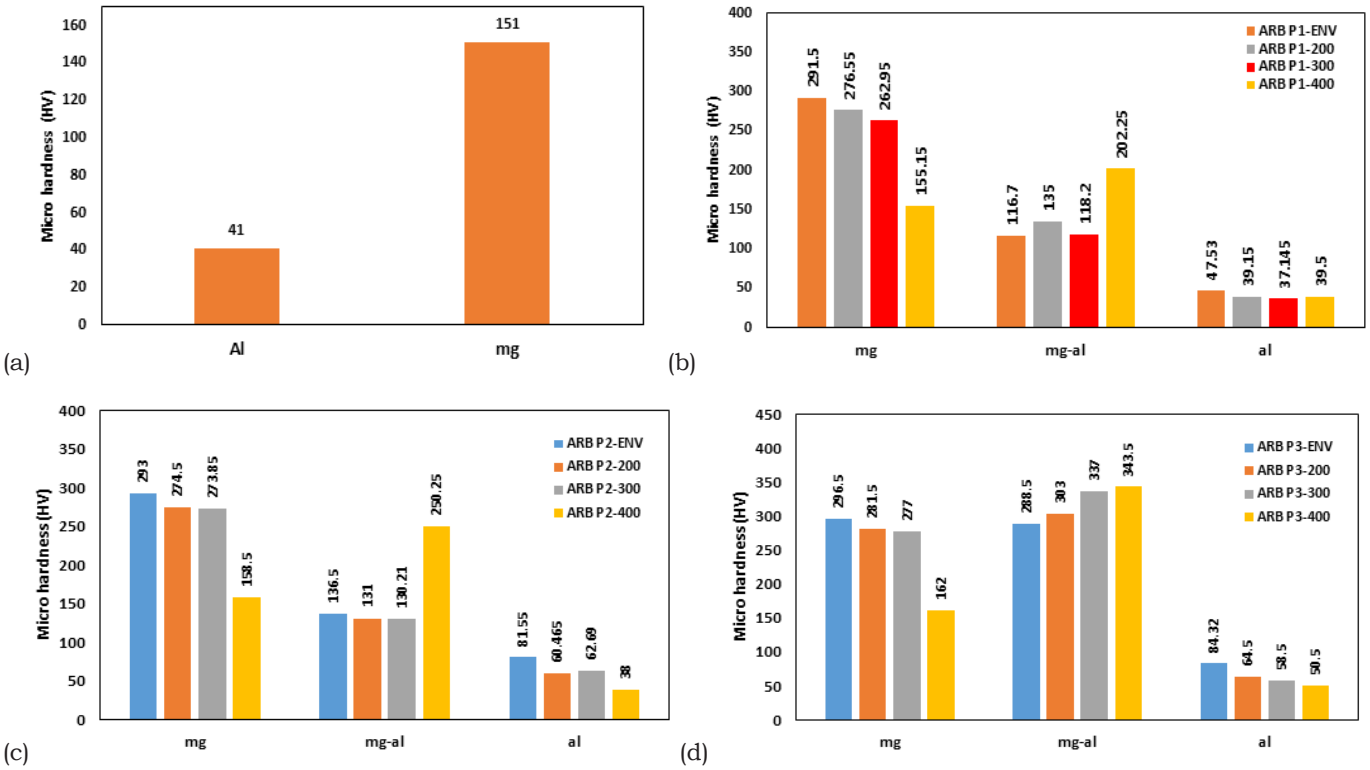

Figure 5: Micro-hardness test results in 4 different temperature conditions: (a) Base sheets, (b) ARB pass 1, (c) ARB pass 2, (d) ARB pass3.

a) As the annealing temperature increases due to the reduction of the work hardening effect, the reduction of the dislocation density, and the growth of grain size in the microstructure, the hardness will decrease.

b) By increasing the annealing temperature, there is a possibility of intermetallic phase formation in the infiltration zone of Al and Mg.

From the above results, it can be seen that if the annealing temperature increases in the non-permeable layers, the hardness decreases due to the decrease in the density of dislocations and the increase in the grain size. However, for the penetration zone, if the secondary phase formed is higher than the hardness of the base metals, then the annealing process will increase the hardness in the penetration zone. An increase in hardness was achieved at the annealing temperature of 400 °C. One of the main reasons for this increase in hardness is the presence of hard secondary phases in this temperature range.

Fracture toughness study

One of the critical parameters that need to be checked in the ARBed samples is fracture toughness. Fracture toughness, like yield stress, is one of the inherent material properties. The fracture toughness test sample was prepared according to the E561-10 standard. This test shows that the energy required until the moment of failure for the ARBed sheets increased or decreased compared to the base sheet. The fracture toughness test results for base and ARBed samples are shown in Figure 6&7, respectively. The results of the fracture toughness are shown in Table 1. By checking Table 1, it can be seen that the increase in ARB passes results in higher toughness. The fracture toughness for the 3-pass ARBed sample compared to the Al and Mg base sheet increased by 50 and 111 percent, respectively. Usually, in mechanical structures, fracture toughness has the opposite relationship with strength. However, the fracture toughness will increase with increasing temperature and strain rate for the metallurgical structure. In order to be able to simultaneously have high fracture toughness in addition to high strength in the sample, it is necessary to strengthen it through microstructure and secondary fine particles. Therefore, in the ARB process, by increasing the number of ARB passes, in addition to obtaining high strength, the fracture toughness will also increase. As stated, the reason for the direct relationship between fracture toughness and strength in the ARBed sample is the fineness of grain structure and the formation of secondary phase particles. The presence of secondary particle phases reduces the chance of accumulating sliding bands, which are places of local stress, which will delay the failure of the sample.

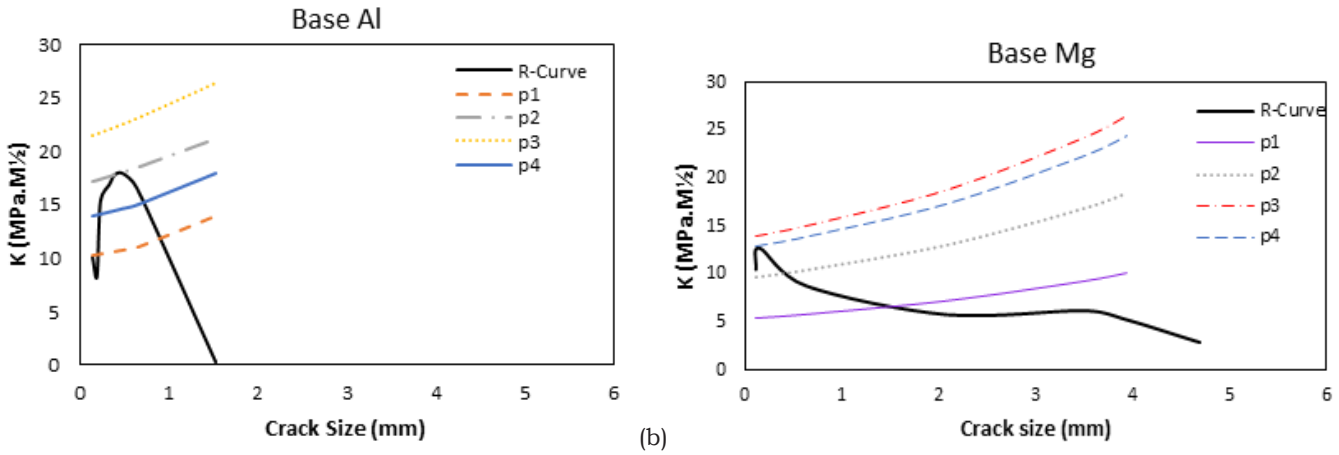

Figure 6: Fracture toughness for base samples, (a) AA 1050, (b) AZ31B.

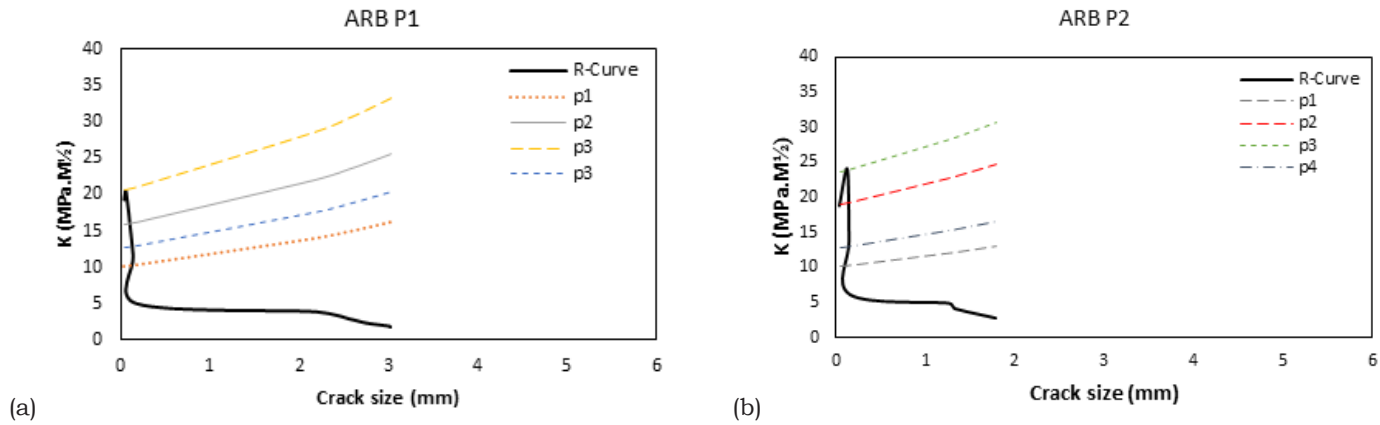

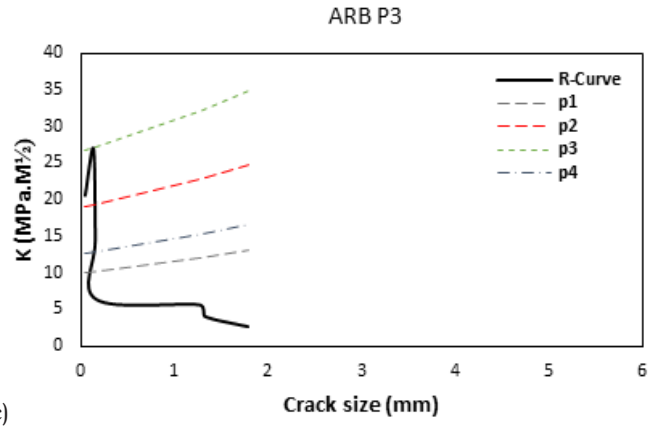

(c)

Figure 7: Fracture toughness for ARB samples, (a) ARB P1, (b) ARB P2, (c) ARB P3.

Table 1: Summary of the fracture toughness test results.

Sample	Fracture Toughness (MPa.M$^{1/2}$)
ARB P1	20.4
ARB P2	24.1
ARB P3	26.95
Al base	17.85
Mg base	12.75

Three-point bending investigation

The three-point bending test was performed to check the layer strength and separation of layers in the ARBed samples, and the results were compared with those of the base sheet. The samples were prepared with a width of 10mm and a length of 100mm. The force-displacement diagram is presented in Figure 8. The results of the bending test show that in the ARBed samples, the bending strength of the sample will grow with the increase in the ARB pass. Also, the 3-point bending test results show that the ARBed samples have good bonding strength between their layers.

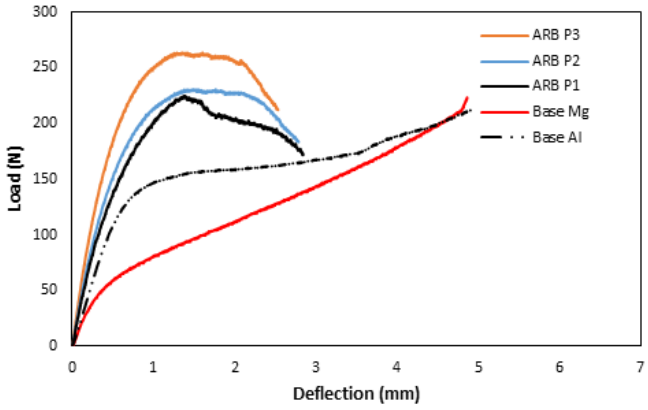

Figure 8: The results of the three-point bending test.

Penetration depth study

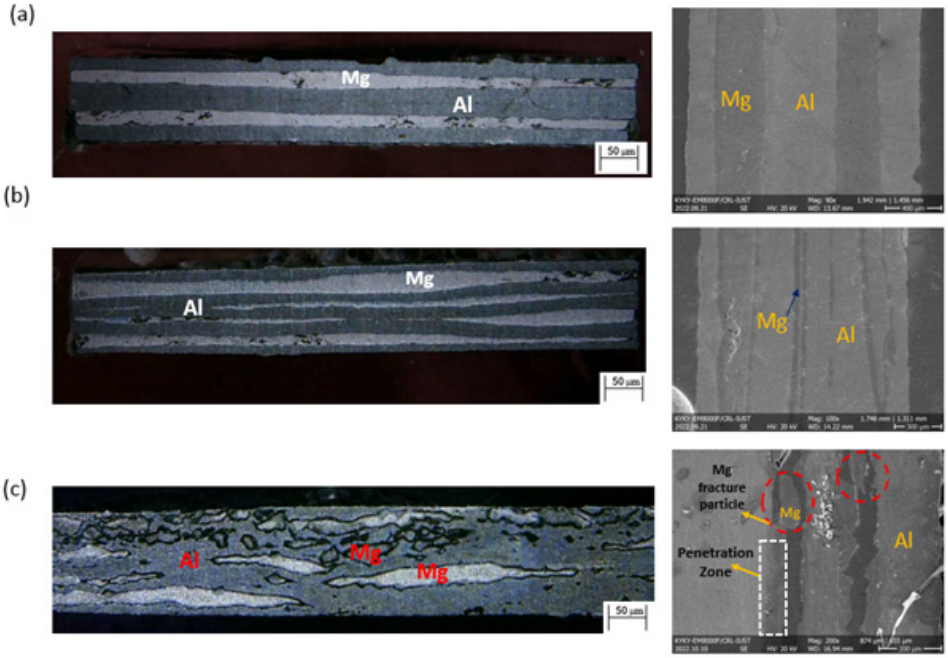

Figure 9: OM and backscatter result for ARB samples, (a) pass 1, (b) pass 2, (c) pass 3.

In Figure 9(c), it is clear that in the third pass, Mg is wholly consumed. One of the essential parameters in producing multilayer composites is the excellent penetration of the layers into each other and good interlayer strength [27]. For this purpose, SEM imaging, EDS-line, and map reports were done for the ARBed samples of passes 1 to 3 in 4 different annealing temperature conditions. In addition to the penetration depth results, the percentage of metals on the composite surface in the three Al regions (A), the penetration region (B) and the Mg region (C) are shown separately in Figures 10-12. Kirkendall's experiments show that the penetration speed of two atoms in a two-component solution is not the same and that the element with a lower melting point penetrates faster [28]. Therefore, due to the proximity of the melting point of Al/Mg, the penetration speed of both is the same. Because one of the most influential parameters in increasing the penetration rate is temperature. With the increase in annealing temperature, the penetration of layers increases [19,20]. As a result, intermetallic phases will be formed in the penetration region. One of the reasons for the increase in penetration depth at higher temperatures can be the surface tension of grain boundaries and the dynamics of grain boundaries at high temperatures. It can be seen that with the increase of temperature in the ARB samples of pass 1 to 3, the gradient of Mg infiltration in Al decreases, which indicates the infiltration of Mg in Al. The reason for this is the decrease in the hardness of Mg and Al and the increase in the contact surface between the surfaces of the base metals [29].

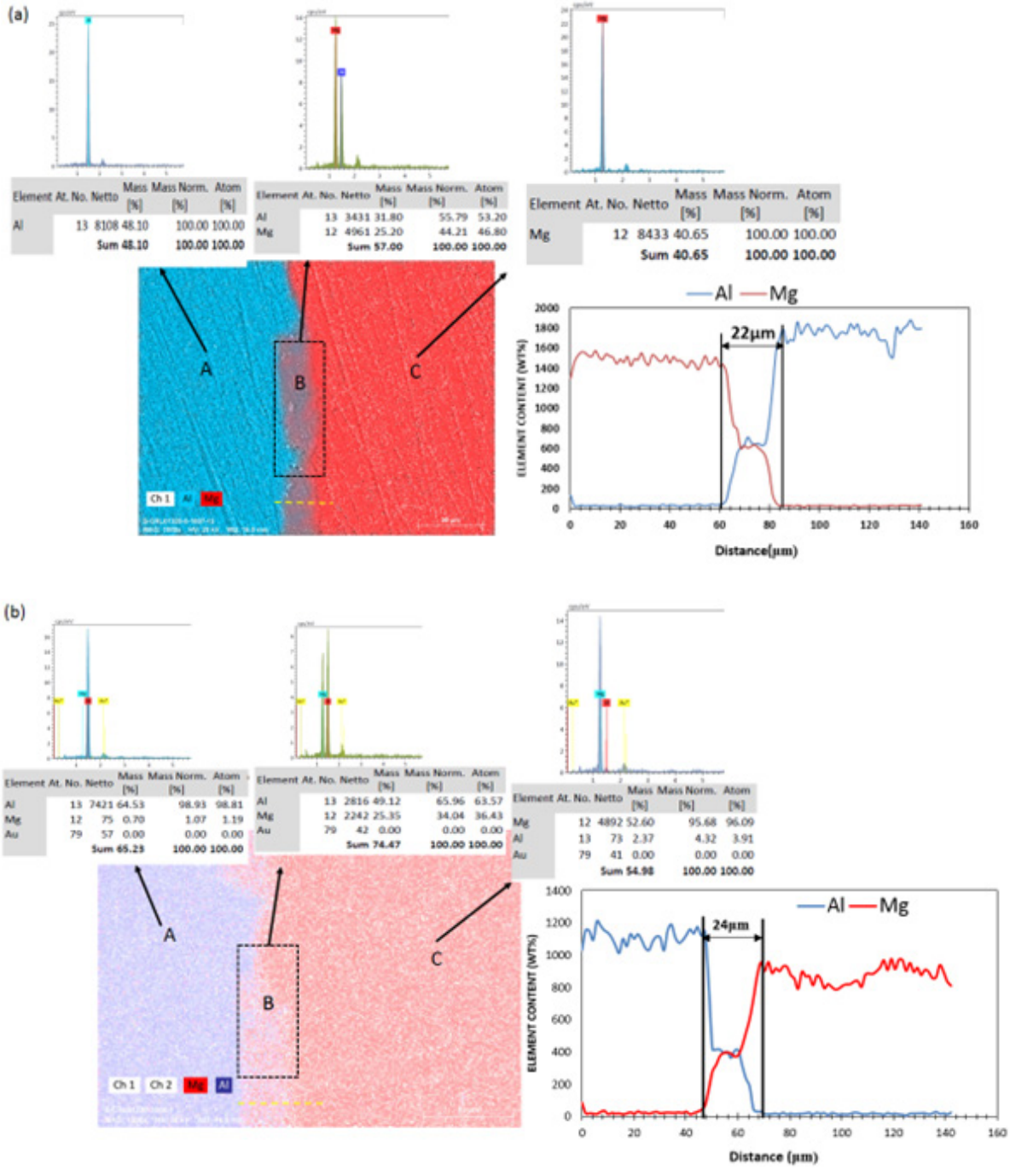

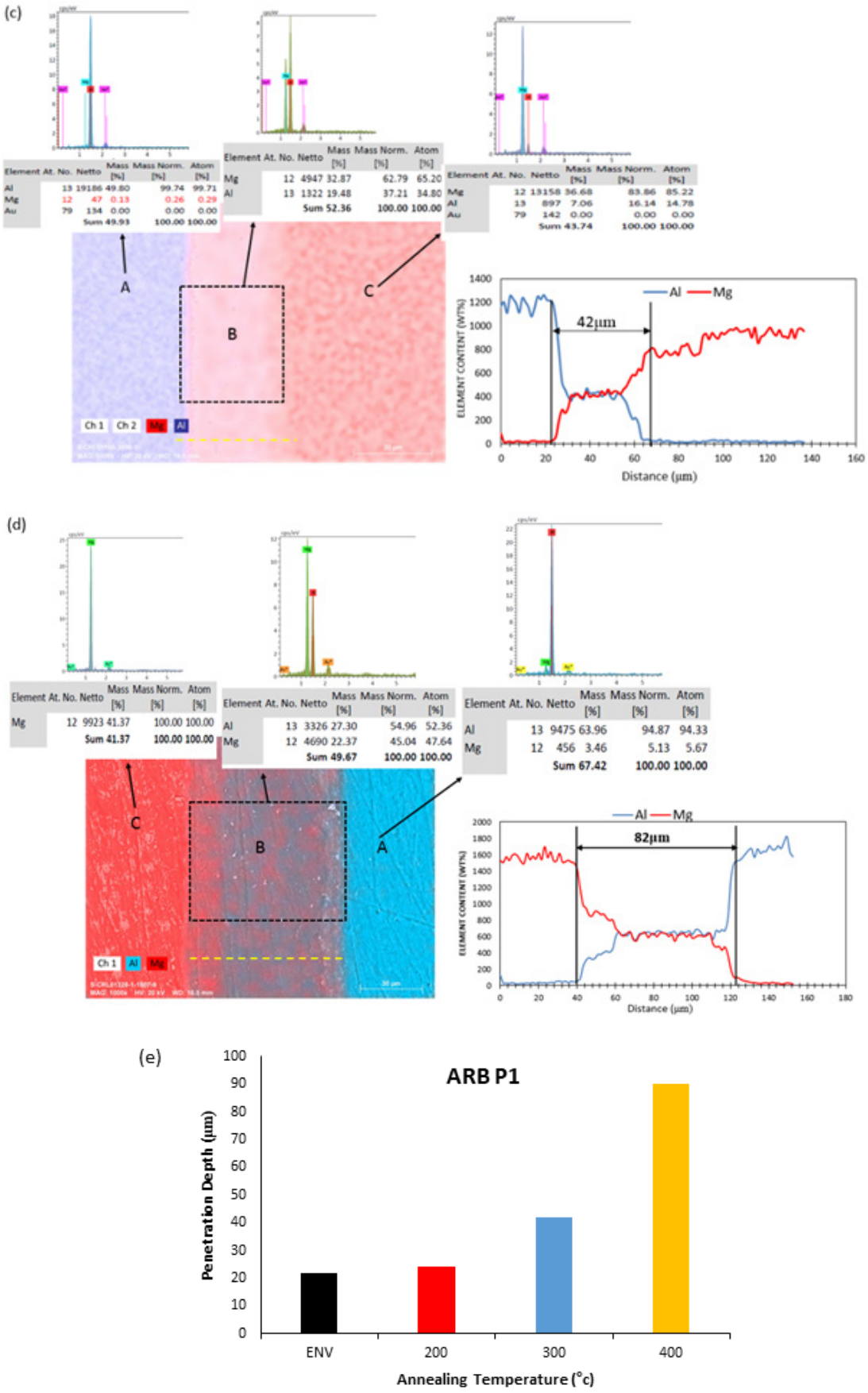

Figure 10: Penetration depth and percentage of elements in areas A, B, and C for the ARBed pass 1, (a) environment temperature,(b) 200°C, (c) 300°C, (d) 400°C, (e) Graph of penetration depth at different annealing temperatures.

(a)

Element	At. No.	Netto	Mass [%]	Mass Norm. [%]	Atom [%]
Mg	12	10083	39.59	100.00	100.00
		Sum	39.59	100.00	100.00

Element	At. No.	Netto	Mass [%]	Mass Norm. [%]	Atom [%]
Mg	12	5884	30.98	51.88	54.48
Al	13	2453	28.73	48.12	45.52
		Sum	59.70	100.00	100.00

Element	At. No.	Netto	Mass [%]	Mass Norm. [%]	Atom [%]
Al	13	11230	51.95	100.00	100.00
		Sum	51.95	100.00	100.00

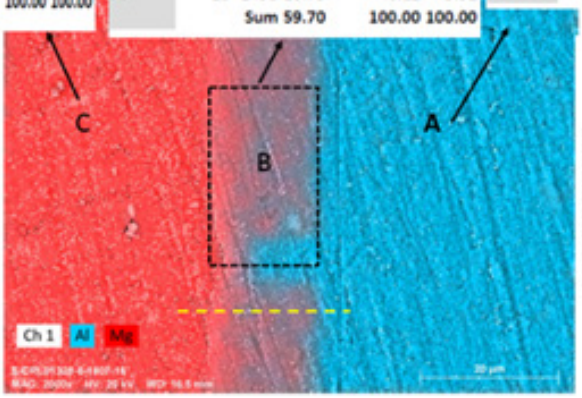

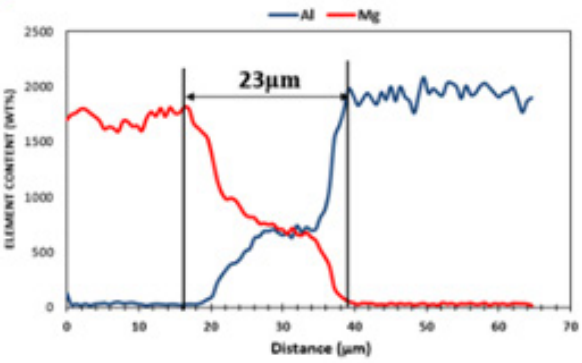

(b)

Element	At. No.	Netto	Mass [%]	Mass Norm. [%]	Atom [%]
Al	13	13821	43.17	99.61	99.57
Mg	12	49	0.17	0.39	0.43
Au	79	194	0.00	0.00	0.00
		Sum	43.34	100.00	100.00

Element	At. No.	Netto	Mass [%]	Mass Norm. [%]	Atom [%]
Al	13	3318	31.96	54.75	52.15
Mg	12	4853	26.41	45.25	47.85
Au	79	139	0.00	0.00	0.00
		Sum	58.37	100.00	100.00

Element	At. No.	Netto	Mass [%]	Mass Norm. [%]	Atom [%]
Mg	12	7209	37.94	94.22	94.76
Al	13	144	2.33	5.78	5.24
Au	79	107	0.00	0.00	0.00
		Sum	40.27	100.00	100.00

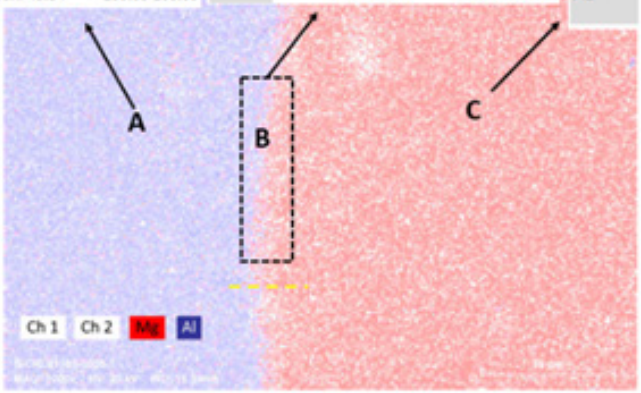

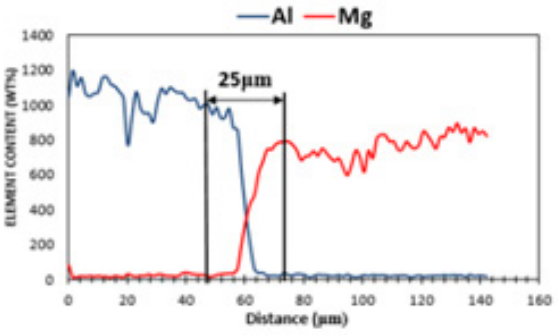

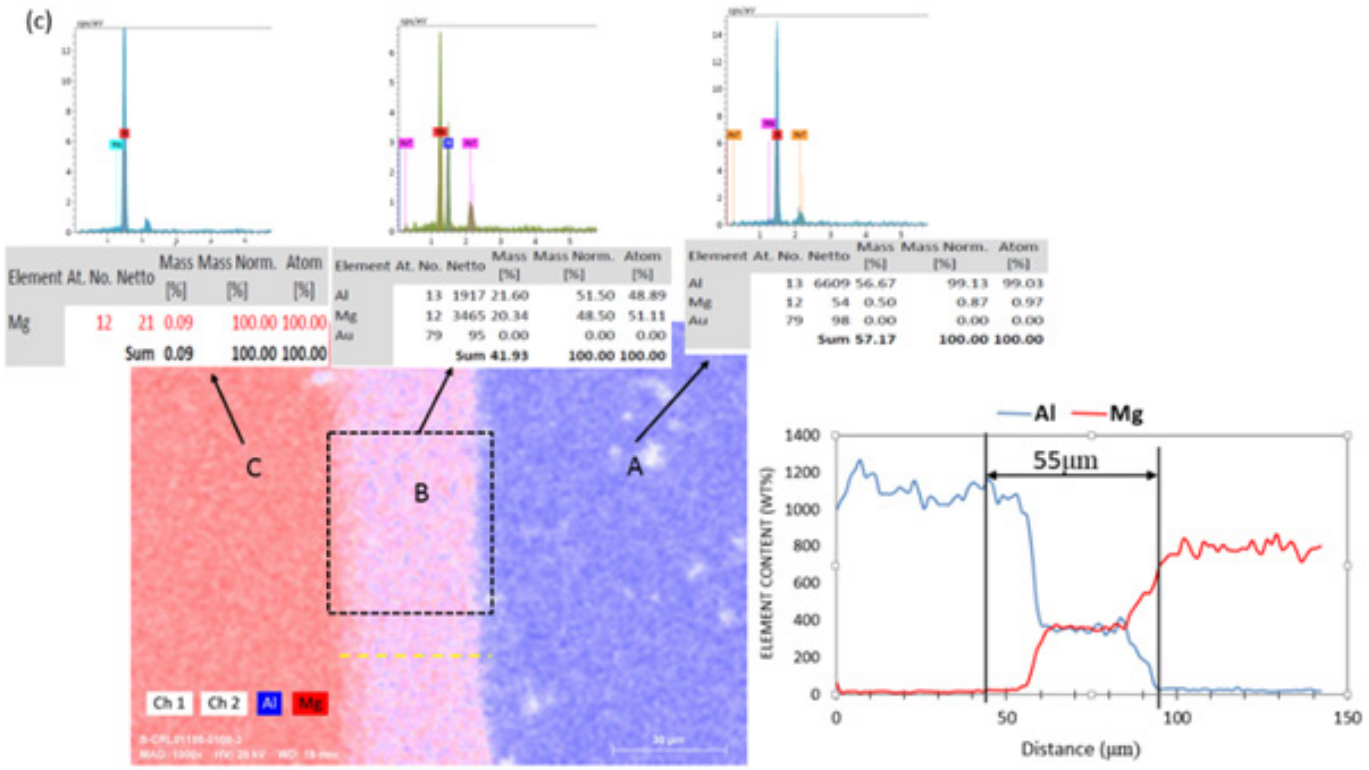

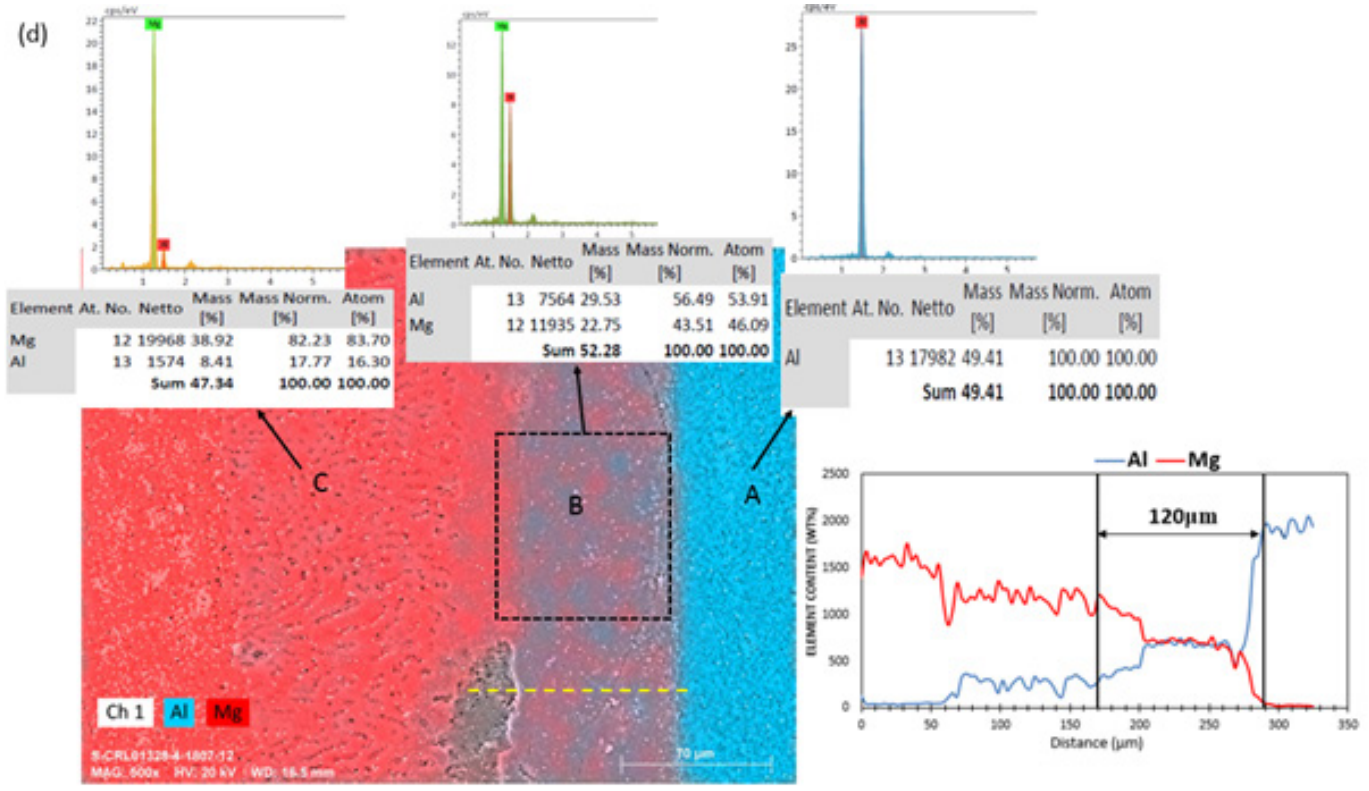

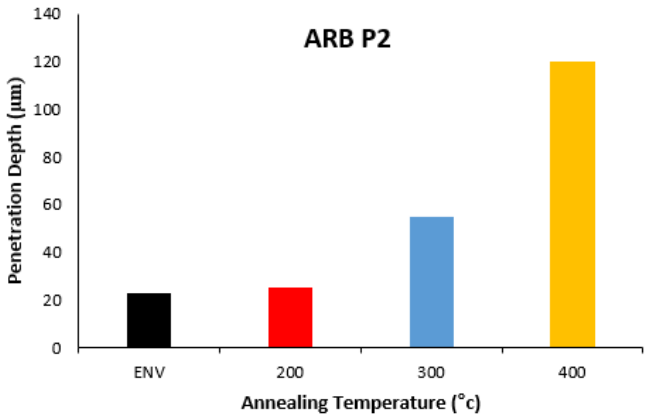

Figure 11: Penetration depth and percentage of elements in areas A, B, and C for the ARBed pass 2, (a) Environment temperature, (b) 200 °C, (c) 300 °C, (d) 400 °C, (e) Graph of penetration depth at different annealing temperatures.

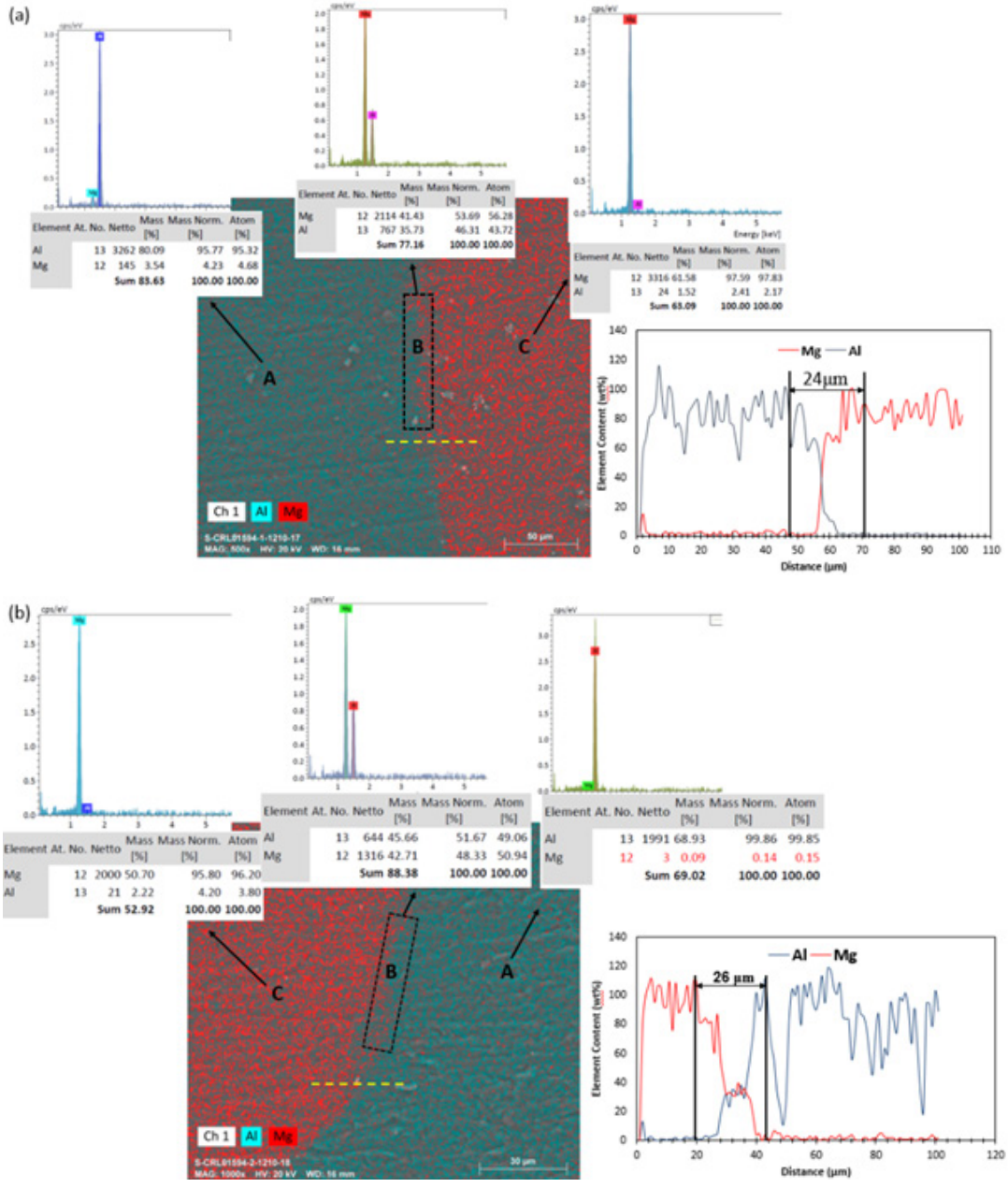

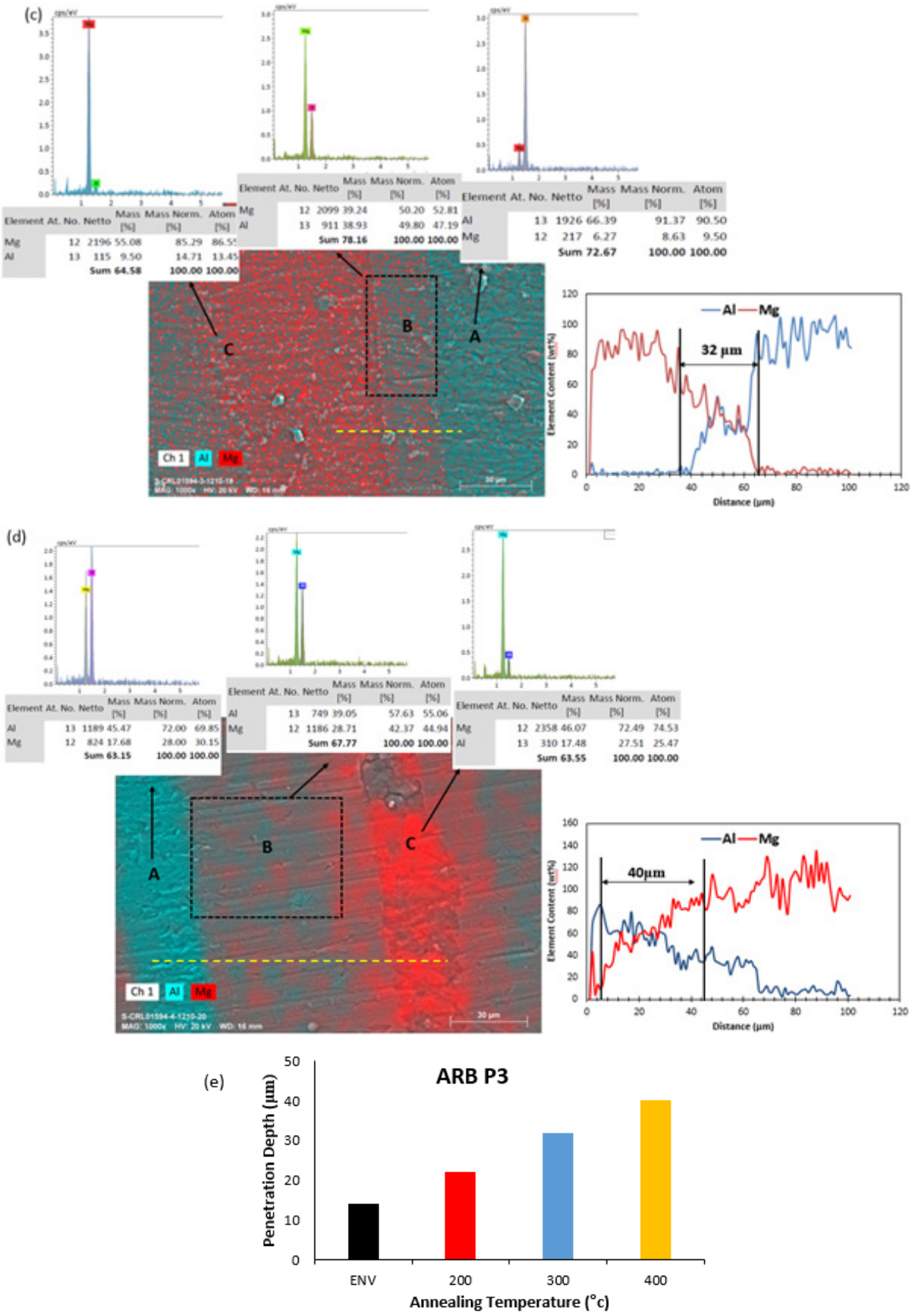

Figure 12: Penetration depth and percentage of elements in areas A, B, and C for the ARBed pass 3, (a) environment temperature, (b) 200 °C, (c) 300 °C, (d) 400 °C, (e) Graph of penetration depth at different annealing temperatures.

XRD result

When the condensation of atoms reaches the level necessary to carry out a chemical reaction, a new composite phase will be formed. The intermetallic phases for the samples ARBed in pass 1 to 3 in 4 different temperature conditions are shown in Figures 13-15. Although the existence of secondary phases has been confirmed by examining Figures 10-12, an XRD test was performed for more detailed investigations [30,31]. In this pattern, several peaks can be seen, some of which are due to the formation of intermetallic compounds, and the others are related to the peaks of Al and Mg base metals. According to the XRD results, four intermetallic phases $Al_{0.58}$ $Mg_{0.42}$, $Al_{12}Mg_{17}$(γ) [20-25], Al_3Mg_2(β) [32] and Al-mg for different temperature conditions can be seen. γ phase has a (Body Center Cubic) Bcc crystal structure and the β phase has an FCC (Face Center Cubic) crystal structure. The possibility of new phase precipitation will depend on factors such as atom penetration state, thermodynamic force, and reaction temperature. New phases nucleate at defects, where the concentration of the infiltrated element is high, and are created along the interface [33]. Because the γ phase is harder than the β phase and the formation of the γ phase at 400° has a higher percentage, the increase in hardness in the penetration zone of the Al/Mg sample can be attributed to the formation of γ phase [34]. Due to the interatomic bonds, the compounds are mainly brittle and, therefore, cause better and more crack propagation. As a result, these compounds can reduce the bond strength of the sheets. In the following, the results obtained from the XRD analysis were analyzed for optimization and microstructural quantitative studies by MAUD software using the Rietveld method. Quantitative results obtained from MAUD software for Crystallite Size and internal micro-strains are shown in Figure 16(a&b), respectively. The results show that with increasing annealing temperature, the crystallite size will increase and the micro-strain will decrease. Considering that in the process of recrystallization, the energy required for grain growth is obtained from the strain energy stored during deformation, therefore, as stated, with increasing annealing temperature, grain growth can be expected in exchange for reducing the internal micro-strain [28]. But the results show that by increasing the ARB pass and increasing the cold work, the grain size and strains will be decrease. Theoretically, it can be observed that with the increase of annealing temperature and recrystallization process, the dislocation density will decrease and as a result, ductility will increase and strength will decrease [33,34]. Using the Eq.1, the dislocation density has been obtained at different annealing temperatures. In Eq.1, Ɛ is the internal micro-strain, d is the crystallite size, and b called the Burgers vector. The results obtained of dislocation density in the Figure 16(c) has been shown [35]. By examining the graph, it is clear that the dislocation density in the ARB sample decreases with the increase of the annealing temperature and it increases with the increase of the ARB pass. Among the reasons for the decrease in the density of dislocations with the increase in the annealing temperature, are the increase in the grain size and the decrease in internal strains and the decrease in residual stresses. The obtained results of the grain size and density of dislocations can validate the results of tensile and hardness tests regarding the decrease in strength with increasing annealing temperature [36].

$$\rho = \frac{2\sqrt{3\varepsilon}}{db} \qquad (1)$$

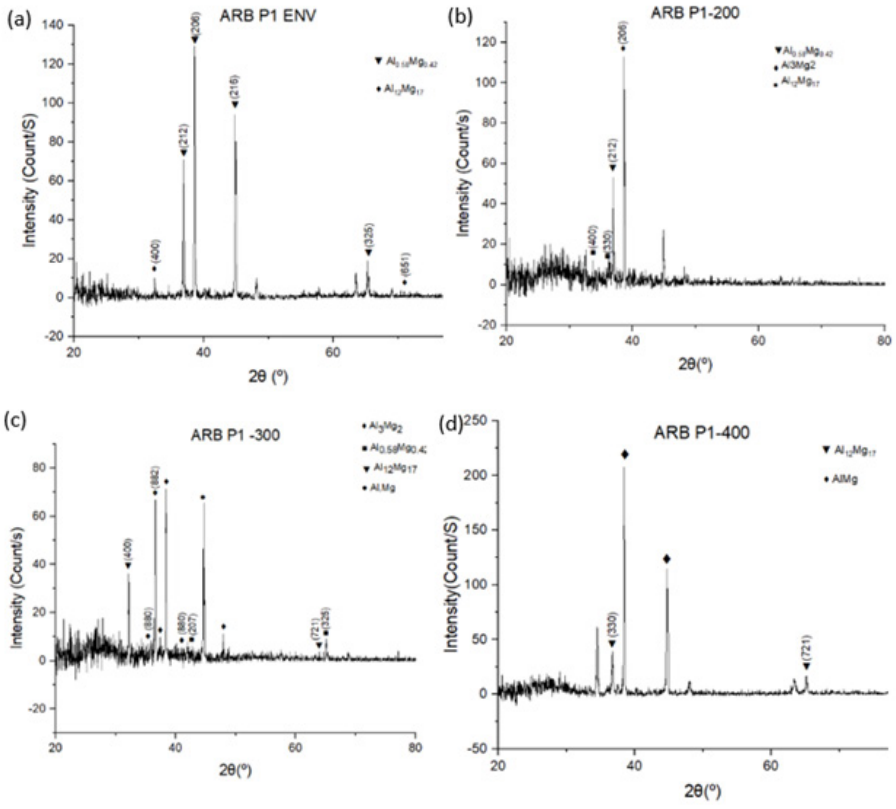

Figure 13: XRD patterns for ARBed sample of first pass, (a) room temperature, (b) 200 °C, (c) 300 °C, (d) 400 °C.

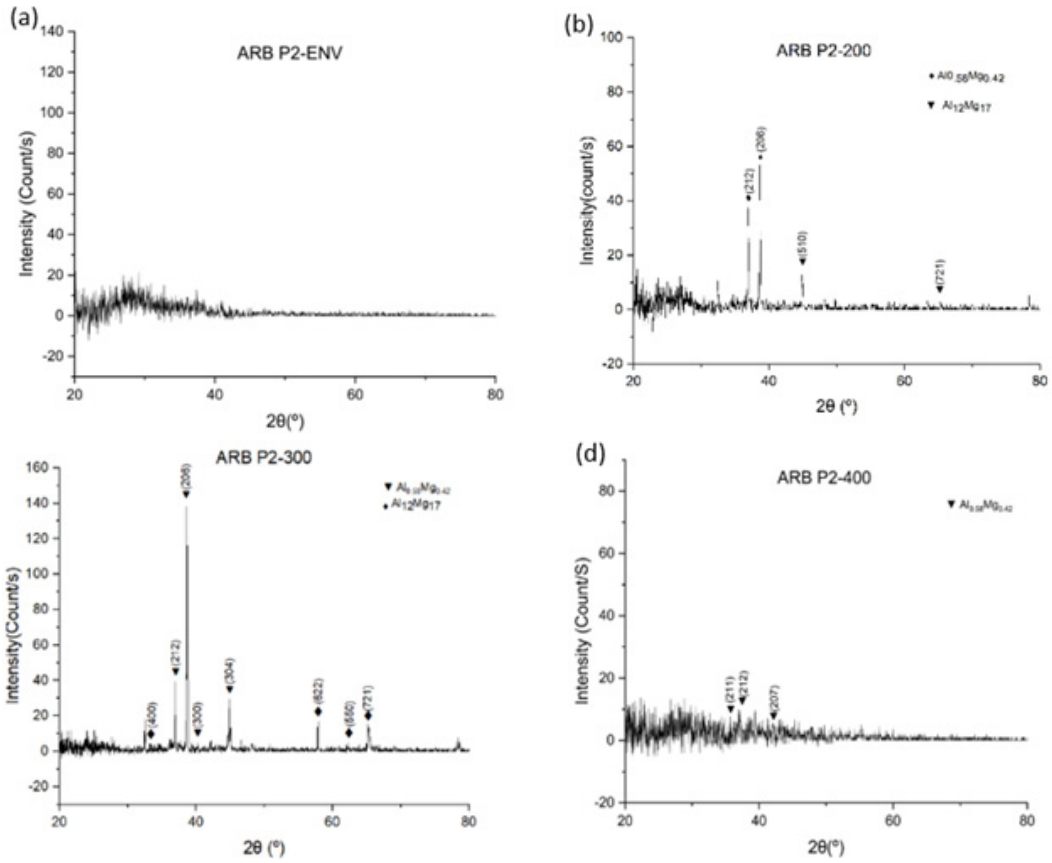

Figure 14: XRD patterns for ARBed sample of second pass, (a) Environment temperature, (b) 200 °C, (c) 300 °C, (d) 400 °C.

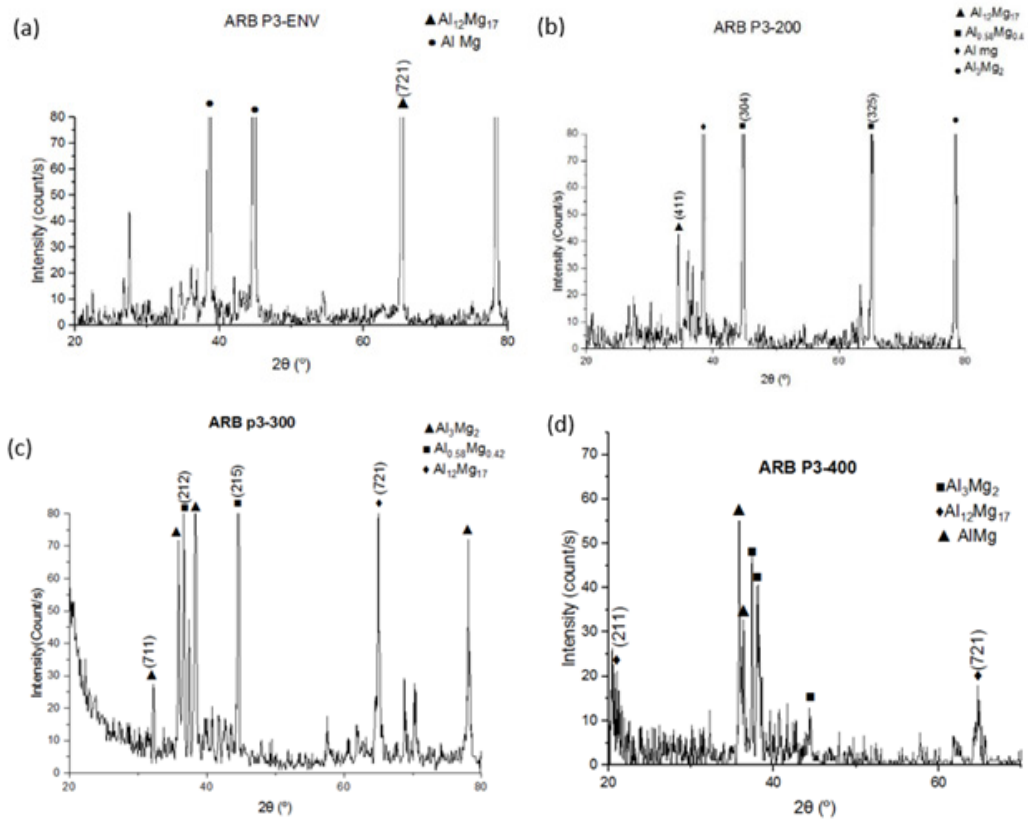

Figure 15: XRD patterns for ARBed sample pass 3, (a) environment temperature, (b) 200 °C, (c) 300 °C, (d) 400 °C.

(a)

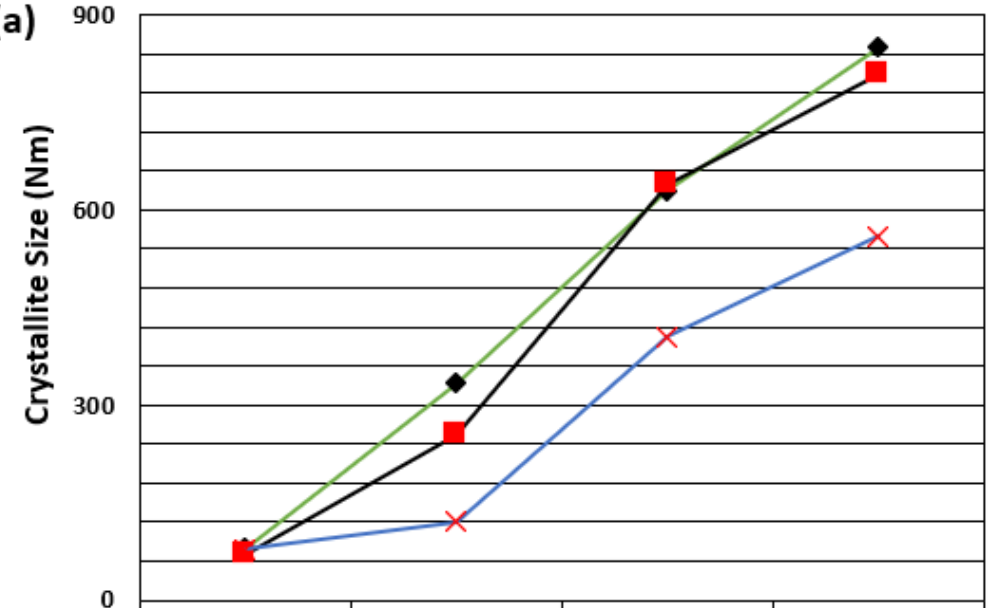

	1	2	3	4
ARB P1	80	333	630	850
ARB P2	71.46	255	640	809
ARB P3	78	120	405	560

Annealing temperature

(b)

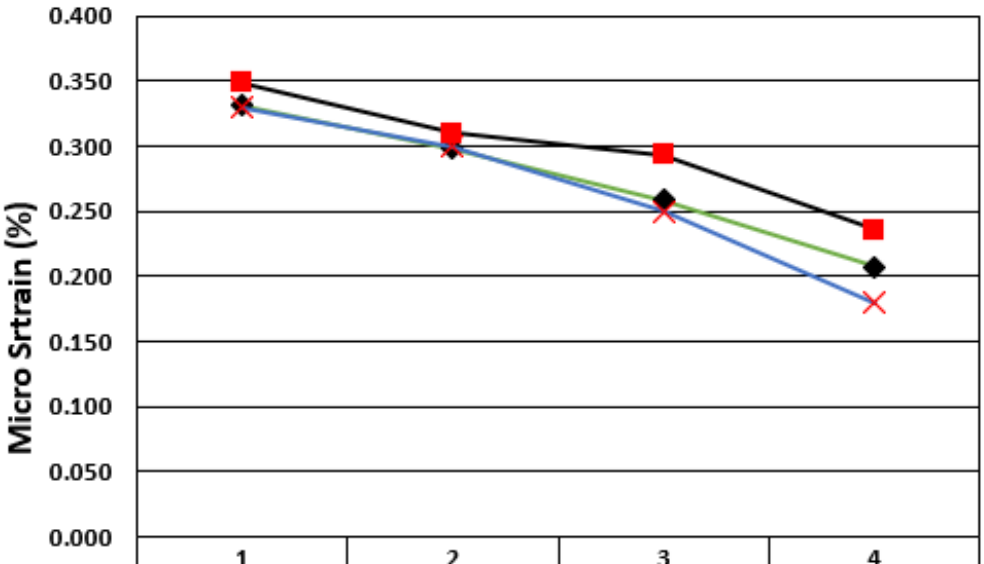

	1	2	3	4
ARB P1	0.331	0.298	0.259	0.207
ARB P2	0.35	0.31	0.29	0.24
ARB P3	0.33	0.3	0.25	0.18

Annealing temperature

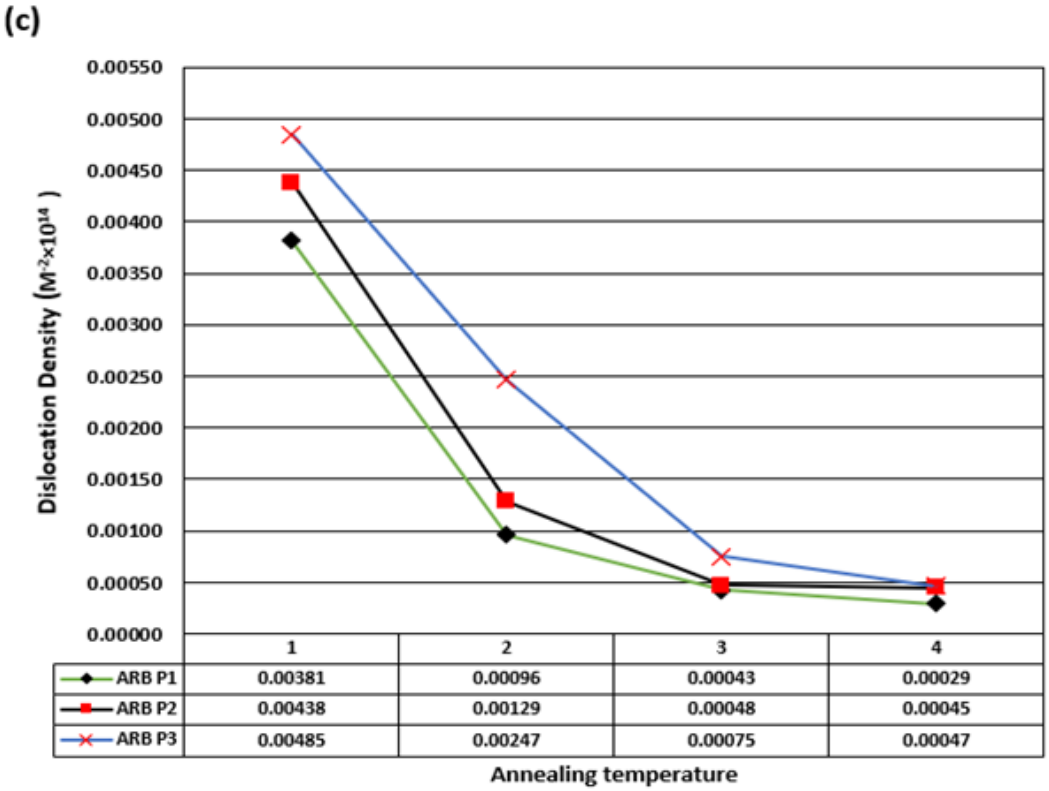

Figure 16: Effect of annealing temperature ARB pass on microstructural properties, (a) Crystallite Size, (b) Micro-Strain, (c) Dislocation density.

Fracture surfaces investigation

Considering that the tensile test was performed for different temperature conditions, it is necessary to check the type of failure in the ARBed samples and the base sheets (Figures 17-20). Different types of failure occur in metals depending on the material, temperature, stress state, and strain rate [37]. In general, there are two types of ductile and brittle fracture mechanisms for metals according to the crystal structure of metals. Brittle fracture is observed more in BCC and HCP metals, but in FCC metals, except for the cases where the factors contributing to grain boundary brittleness, the fracture will be ductile [38]. In brittle metals, the type of fracture is strongly dependent on temperature. At low temperatures, the fracture is brittle; at high temperatures, the fracture will occur in a soft mode. Therefore, with increasing temperature, the transition from brittle to soft behavior will occur. Brittle fracture is more possible at low temperatures because the critical shear stress component for the sliding of shear plates will occur at higher stresses [39]. One of the causes of brittle failure is the presence of secondary phases. By examining Figures 13-15 the presence of secondary particles was proved for samples rolled at different temperatures.

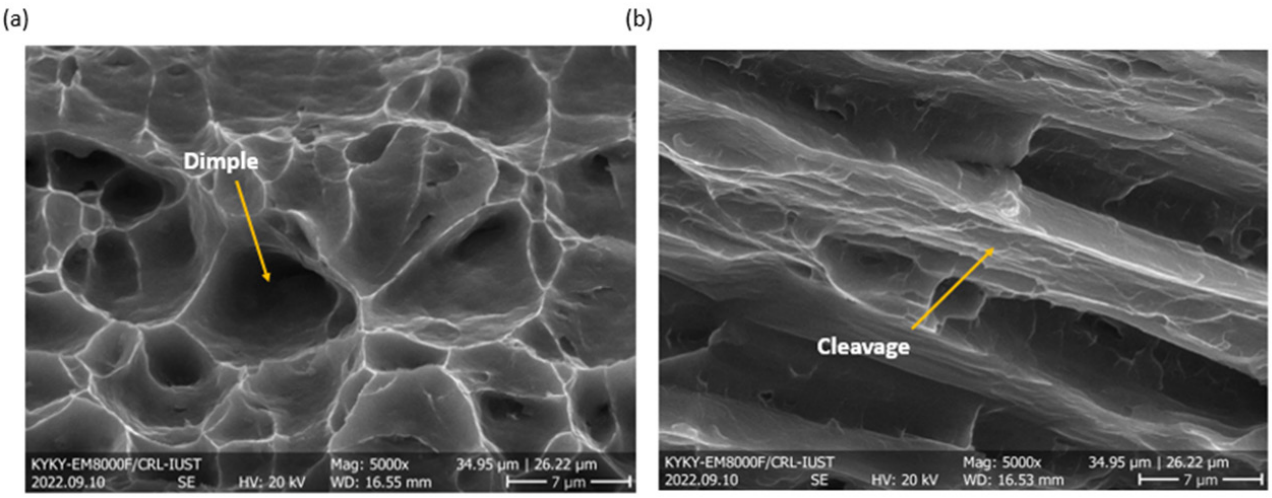

Figure 17: SEM images fracture surfaces after tensile test, (a) Al base sheet, (b) Mg base sheet.

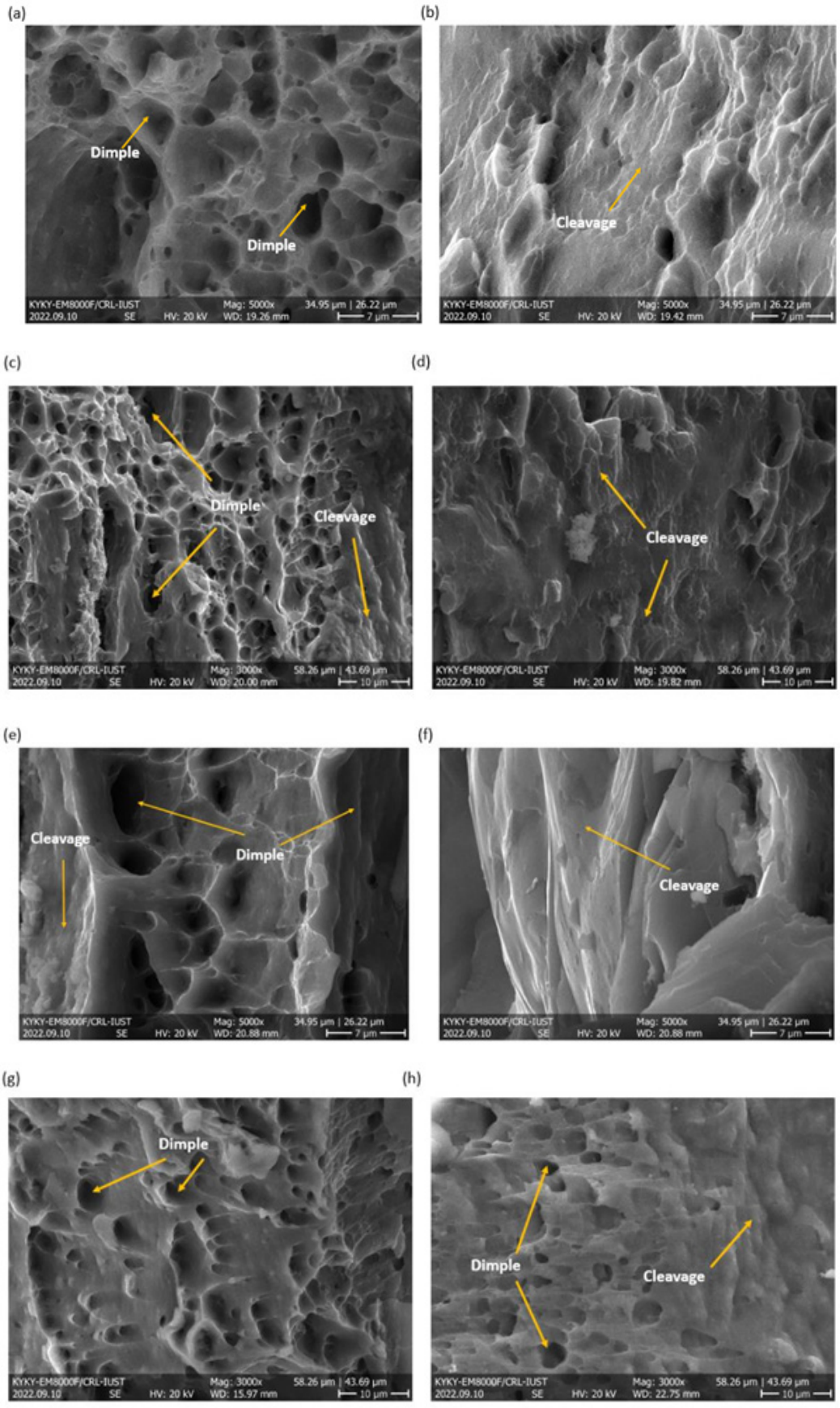

Figure 18: SEM images of the ARB pass one fracture surfaces after tensile test, (a) Al at an environment temperature, (b) Mg at an environment temperature, (c) Al at a 200 °C, (d) Mg at a 200 °C, (e) Al at a 300 °C, (f) Mg at a 300 °C, (g) Al at a 400 °C, (h) Mg at a 400 °C.

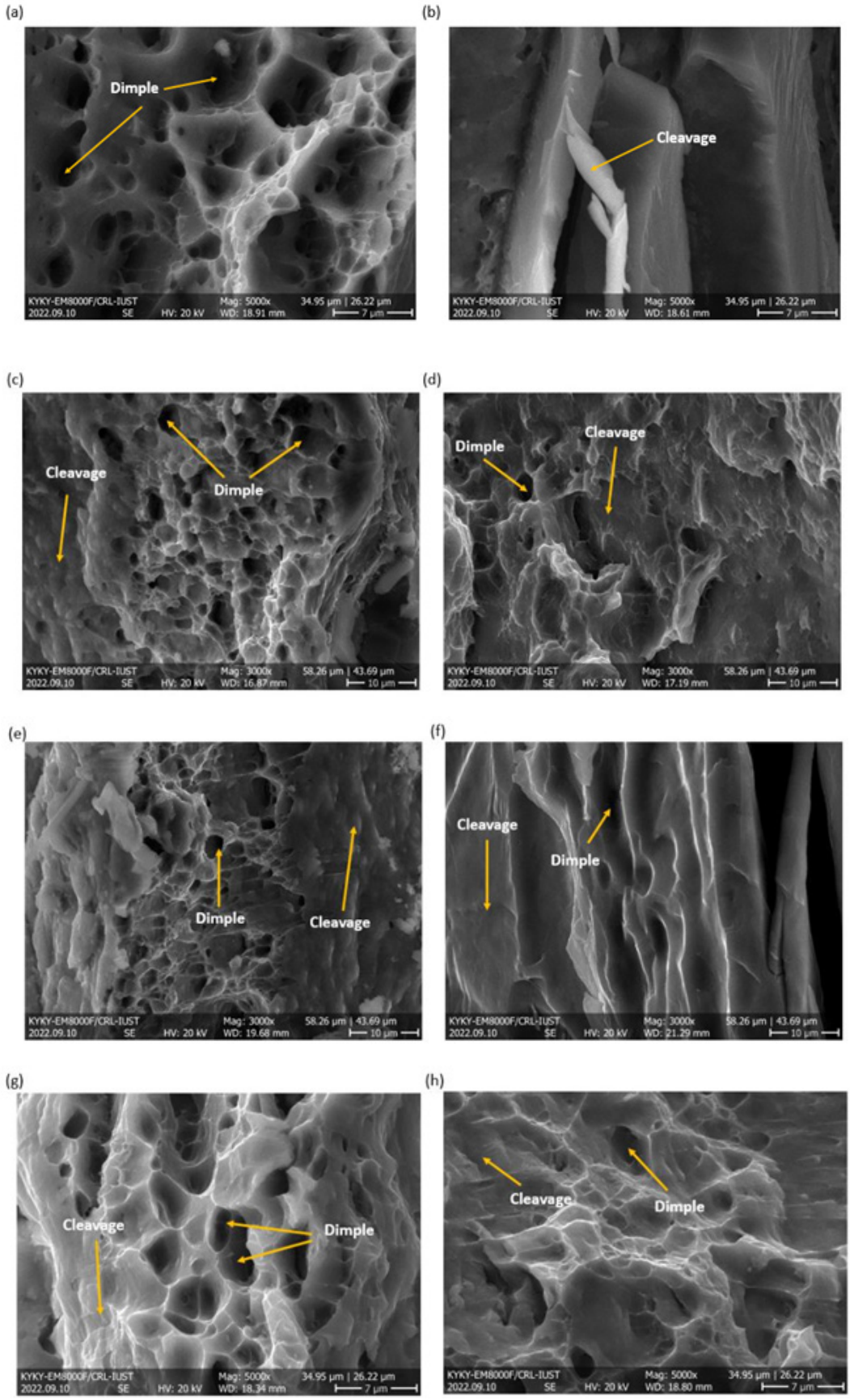

Figure 19: SEM images of the ARB pass one fracture surfaces after tensile test, (a) Al at an environment temperature, (b) Mg at an environment temperature, (c) Al at a 200 °C, (d) Mg at a 200 °C, (e) Al at a 300 °C, (f) Mg at a 300 °C, (g) Al at a 400 °C, (h) Mg at a 400 °C.

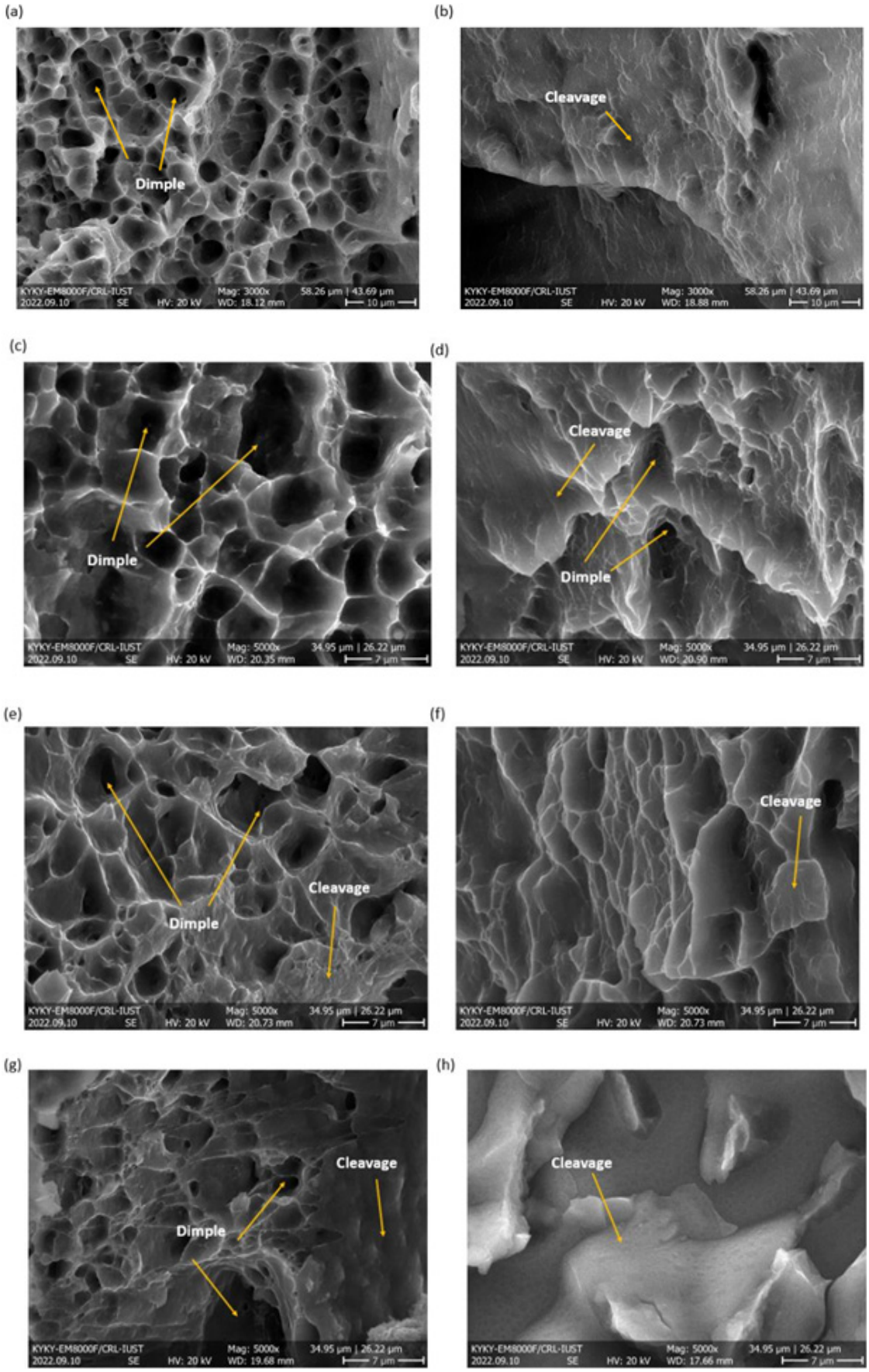

Figure 20: SEM images of the ARB pass three fracture surfaces after tensile test, (a) Al at an environment temperature, (b) Mg at an environment temperature, (c) Al at a 200 °C, (d) Mg at a 200 °C, (e) Al at a 300 °C, (f) Mg at a 300 °C, (g) Al at a 400 °C, (h) Mg at a 400 °C.

On the other hand, the presence and nature of secondary phase particles significantly affect the initiation of micro-cracks. Analyses related to the fracture in the ARB first pass in Figure 18 have been shown. Fracture analysis at ambient temperature indicates brittle and ductile fracture for Mg and Al regions, respectively. Nevertheless, different conditions have happened for annealing temperatures of 200, 300, and 400 °C and in the annealing temperature of 200 °C, brittle fracture occurred in the Mg region. Nevertheless, in the Al area, the fracture happened in a combination of brittle and ductile, which indicates the dominance of the intermetallic effect phases on the annealing temperature. This incident has also been repeated at an annealing temperature of 300 °C. However, at the annealing temperature of 400 °C, the effect of the annealing temperature overcame the intermetallic phases, and the fracture mechanism in the Mg region is ductile and brittle. In the Al region, it occurred in a ductile form with shallow dimples. Analyses related to the fracture in the ARB second pass in Figure 19 have been shown. In the ARB from the second pass onwards, due to the break of the Mg layer structure, it is difficult to distinguish the fracture surface for the Mg and Al layers. For the ARB Mg layer in the second pass at ambient temperature, the Mg layer is broken, but its surface shows a brittle fracture. For the Al layer, the failure occurred as a combination of ductile and brittle. For other annealing temperatures, the fracture mechanism for Mg and Al regions is a combination of brittle and ductile. However, it can be seen that for the Mg region, the primary phenomenon of fracture is the brittle mechanism. For the Al region, the primary phenomenon of fracture is ductile fracture. The results of the fracture surface for the ARB samples of the third pass in Figure 20 have been shown. The results for ambient temperature indicate that the fracture is brittle for the Mg layer and ductile for the Al layer. For the annealing temperature of 200 °C in the Mg layer, the fracture mechanism combines brittle and ductile, and most of the fracture mechanism is brittle. The change in the fracture mechanism at this temperature for the Mg layer indicates that the annealing temperature is more effective than the intermetallic phases. However, for the annealing temperature of 300 and 400 °C, there was no mechanical change in the fracture of the Mg layer, but at the annealing temperature of 300 and 400 °C of the Al layer, the fracture mechanism is a combination of ductile and brittle, which is the dominant mechanism of ductile fracture. The presence of a brittle composition in the grain boundary will accelerate the formation of micro-cracks; as a result, the cause of simultaneous brittle and ductile fracture in the Al layer structure at 300 °C and 400 °C in the first and second pass of the ARB process can be considered to be the presence of a secondary phase in the grain boundary.

Conclusion

The ARB process was used to fabricate the AA 1050/Mg AZ31B sheets until the third pass. The effect of the ARB process on the composite was investigated by examining the mechanical and metallurgical properties of the produced samples. The obtained results can be summarized as follows:

A. EDS-Line and map analysis showed that with the increase in annealing temperature, the depth of the penetration layer will also increase for ARB samples.

B. The tensile test showed that the strength of the ARB sample in the third pass increased by about 250% compared to the aluminum base metal, and it decreased by about 10% compared to the Mg base metal. Also, increasing the annealing temperature will decrease the strength and increase the ductility in the ARB samples.

C. The hardness test results show an increase in the hardness of the ARB sample compared to the base sheet. However, due to a hard secondary phase at an annealing temperature of 400 degrees, the hardness has increased in the penetration zone.

D. The fracture toughness for the ARBed samples was performed up to the third pass and compared with the base sheet results. The results showed that with the increase in the ARB passes, the fracture toughness also increases.

E. The analysis of the results of the fracture test showed that the ARB samples in the Al region, at 300° and 400° annealing temperatures, due to the formation of intermetallic phases, a change in fracture mode occurred for them from a soft fracture state to a brittle-soft mode.

Acknowledgment

This work is based upon research funded by the Iran National Science Foundation (INSF) under project No. 4005147.

References

1. Romhanji E, Popović M, Glišić D, Stefanović M, Milovanović M (2004) On the Al-Mg alloy sheets for automotive application: Problems and solutions. Bull Mater Sci 10: 205-216.
2. James M, Kihiu JM, Rading GO, Kimotho JK (2011) Use of magnesium alloys in optimizing the weight of automobile: Current trends and opportunities, pp. 4-6.
3. Liu F, Liang W, Li X, Zhao X, Zhang Y, et al. (2008) Improvement of corrosion resistance of pure magnesium via vacuum pack treatment. J Alloys Compd 461(1-2): 399-403.
4. Amirkhanlou S, Rahimian M, Ketabchi M, Parvin N, Yaghinali P (2016) Strengthening mechanisms in nanostructured Al/SiCp composite manufactured by accumulative press bonding. Metall Mater Trans A Phys Metall Mater Sci 47: 5136-5145.
5. Saito Y, Utsunomiya H, Tsuji N, Sakai T (1999) Novel ultra-high straining process for bulk materials development of the Accumulative Roll-Bonding (ARB) process. Acta Mater 47(2): 579-583.
6. Jamaati R, Toroghinejad MR (2010) Manufacturing of high-strength aluminum/alumina composite by accumulative roll bonding. Mater Sci Eng A 527(16-17): 4146-4151.
7. Sarvi Z, Sadeghi A, Mosavi Mashhadi M, Guo B (2022) Effect of Accumulative Roll Bonding (ARB) strain path on microstructural evolution and crystallographic texture development in aluminium. J Mater Res Technol 21: 1061-1071.
8. Cheepu M, Haribabu S, Ramachandraiah T, Srinivas B, Venkateswarulu D, et al. (2018) Fabrication and analysis of accumulative roll bonding process between magnesium and aluminum multi-layers. Appl Mech Mater 877: 183-189.
9. Habila W, Azzeddine H, Mehdi B, Tirsatine K, Baudin T, et al. (2019) Investigation of microstructure and texture evolution of a Mg/Al laminated composite elaborated by accumulative roll bonding. Mater Charact 147: 242-252.
10. Chen MC, Hsieh HC, Wu W (2006) The evolution of microstructures and mechanical properties during accumulative roll bonding of Al/Mg composite. J Alloys Compd 416(1-2): 169-172.

11. Wu K, Chang H, Maawad E, Gan WM, Brokmeier HG, et al. (2010) Microstructure and mechanical properties of the Mg/Al laminated composite fabricated by Accumulative Roll Bonding (ARB). Mater Sci Eng A 527(13-14): 3073-3078.

12. Chang H, Zheng MY, Xu C, Fan GD, Brokmeier HG, et al. (2012) Microstructure and mechanical properties of the Mg/Al multilayer fabricated by Accumulative Roll Bonding (ARB) at ambient temperature. Mater Sci Eng A 543: 249-256.

13. Liu HS, Zhang B, Zhang GP (2011) Microstructures and mechanical properties of Al/Mg Alloy multilayered composites produced by accumulative roll bonding. J Mater Sci Technol 27(1): 15-21.

14. Weiying W, Weiwei Z, Shunli H, Xinmin C, Bingyi Y, et al. (2022) Mechanism of optimization strength-plasticity through matrix microstructure evolution during Mg/Al composite plate by hard-plate accumulative roll bonding. The Lancent Pschch 11: 133-143.

15. Zhang AX, Li F, Huo P Da, Niu WT, Gao RH (2023) Response mechanism of matrix microstructure evolution and mechanical behavior to Mg/Al composite plate by hard-plate accumulative roll bonding. J Mater Res Technol 23: 3312-3321.

16. Alizadeh M, Faramarz V, Shima P (2023) Feasibility study of producing Al-5Zn-1 Mg alloy by accumulative roll bonding process and subsequent heat treatment. Eng Fail Anal 143: 06927.

17. Taherian MM, Yousefpour M, Borhani E (2020) The effect of ARB process on corrosion behavior of nanostructured aluminum alloys in $Na_2HPO_4 \cdot 12H_2O$ and $Zn(NO_3)_2 \cdot 6H_2O$ PCMs. Eng Fail Anal 107: 104222.

18. Esmaeil Zadeh M, Ghalandari L, Sani R, Jafari E (2023) Microstructural evaluation, mechanical properties, and corrosion behavior of the Al/Cu/Brass multilayered composite produced by the ARB process. Met Mater Int 30: 1123-1144.

19. Sun Q, Zhang D, Tong X, Lin J, Li Y, et al. (2024) Mechanical properties, corrosion behavior and cytotoxicity of biodegradable Zn/Mg multilayered composites prepared by accumulative roll bonding process. Acta Biomater 173: 509-525.

20. Jalali A, Hashemi R, Rajabi M, Tayebi P (2022) Finite element simulations and experimental verifications for forming limit curve determination of two-layer aluminum/brass sheets considering the incremental forming process. Proc Inst Mech Eng Part L J Mater Des Appl 236(2): 361-373.

21. Jinfeng Nie, Mingxing Liu, Fang Wang, Yonghao Zhao, Yusheng Li YC et al. (2016) Fabrication of Al/Mg/Al composites via Accumulative Roll Bonding and Their Mechanical Properties. Materials (Basel) 9(11): 951.

22. Jamaati R, Toroghinejad MR (2010) Effect of friction, annealing conditions and hardness on the bond strength of Al/Al strips produced by cold roll bonding process. Mater Des 31: 4508-4513.

23. Payam Tayebi, Amir Reza Nasirin, Akbari H, Rahim H (2024) Experimental and numerical investigation of forming limit diagrams during single point incremental forming for Al/Cu. Metals (Basel) 14(2): 214.

24. ASTM E647-15e1 (2023) Standard test method for measurement of fatigue crack growth rates. Am Soc Test Mater 1-50.

25. Tayebi P, Hashemi R (2024) Study of single point incremental forming limits of Al 1050/Mg-AZ31B two-layer sheets fabricated by roll bonding technique: Finite element simulation and experiment. J Mater Res Technol 29: 149-69.

26. Peng XK, Wuhrer R, Heness G, Yeung WY (1999) On the interface development and fracture behavior of roll bonded copper/aluminum metal laminates. J Mater Sci 34: 2029-2038.

27. Abbasi M, Toroghinejad MR (2010) Effects of processing parameters on the bond strength of Cu/Cu roll-bonded strips. J Mater Process Technol 210(3): 560-563.

28. Reza Abbaschian, Robert E Reed HLA (2009) Physical metallurgy principles. (4th edn), Affiliated East-West Press, Delhi, India, p. 200.

29. Atifeh SM, Rouzbeh A, Hashemi R, Sedighi M (2022) Effect of annealing on formability and mechanical properties of AA1050/Mg-AZ31B bilayer sheets fabricated by explosive welding method. Int J Adv Manuf Technol 118: 775-784.

30. Wang Y, Luo G, Zhang J, Shen Q, Zhang L (2013) Microstructure and mechanical properties of diffusion-bonded Mg-Al joints using silver film as interlayer. Mater Sci Eng A 559: 868-874.

31. Rahmatabadi D, Tayyebi M, Najafizadeh N, Hashemi R, et al. (2021) The influence of post-annealing and ultrasonic vibration on the formability of multilayered Al5052/MgAZ31B composite. Mater Sci Technol (United Kingdom) 37(1): 78-85.

32. Jafarian M, Rizi MS, Javadinejad R, Ghaheri A, Taghi M (2016) Effect of thermal tempering on microstructure and mechanical properties of Mg-AZ31/Al-6061 diffusion bonding. Mater Sci Eng A 666: 372-379.

33. Mahendran G, Balasubramanian V, Senthilvelan T (2009) Developing diffusion bonding windows for joining AZ31B magnesium-AA2024 aluminum alloys. Mater Des 30(4): 1240-1244.

34. Mehr V Yousefi, Mohammad RT (2022) On the texture evolution of aluminum-based composites manufactured by ARB process: A review. J Mater Res Technol 21: 1095-1109.

35. Gu L, Meng A, Chen X, Zhao Y (2023) Simultaneously enhancing strength and ductility of HCP titanium via multi-modal grain induced extra< c+a> dislocation hardening. Acta Mater 252: 118949.

36. Tayebi P, Hashemi R (2024) Study of single point incremental forming limits of Al 1050/Mg-AZ31B two-layer sheets fabricated by roll bonding technique: Finite element simulation and experiment. J Mater Res Technol 29: 149-69.

37. Nie H, Liang W, Chen H, Wang F, Li T, et al. (2019) A coupled EBSD/TEM study on the interfacial structure of Al/Mg/Al laminates. J Alloys Compd 781: 696-701.

38. Bencherifa I, Baya Alili, Thierry Baudin, François Brisset, Dominique T, et al. (2023) On the microstructure and texture of inter metallics in Al/Mg/Al multi-layer composite fabricated by accumulative roll bonding. Micron 173: 103507.

39. Dieter GE (1961) Mechanical metallurgy. (3rd edn), McGraw-Hill, New York, USA, p. 776.